DYNAMIC STIFFNESS MATRIX OF A RECTANGULAR PLATE FOR THE GENERAL CASE

J.R. Banerjee[a*], S.O. Papkov[b], X. Liu[a], D. Kennedy[c]

[a]School of Engineering and Mathematical Sciences, City University London, London EC1V 0HB, UK

[b]Department of Mathematics, Sevastopol National Technical University, Sevastopol 99053, Ukraine

[c]School of Engineering, Cardiff University, Cardiff CF24 3AA, Wales, UK

Abstract

The dynamic stiffness matrix of a rectangular plate for the most general case is developed by solving the bi-harmonic equation and finally casting the solution in terms of the force-displacement relationship of the freely vibrating plate. Essentially the frequency dependent dynamic stiffness matrix of the plate when all its sides are free is derived, making it possible to achieve exact solution for free vibration of plates or plate assemblies with any boundary conditions. Previous research on the dynamic stiffness formulation of a plate was restricted to the special case when the two opposite sides of the plate are simply supported. This restriction is quite severe and made the general purpose application of the dynamic stiffness method impossible. The theory developed in this paper overcomes this long-lasting restriction. The research carried out here is basically fundamental in that the bi-harmonic equation which governs the free vibratory motion of a plate in harmonic oscillation is solved in an exact sense, leading to the development of the dynamic stiffness method. It is significant that the ingeniously sought solution presented in this paper is completely general, covering all possible cases of elastic deformations of the plate. The Wittrick-Williams algorithm is applied to the ensuing dynamic stiffness matrix to provide solutions for some representative problems. A carefully selected sample of mode shapes is also presented.

Keywords: Dynamic stiffness method; free vibration; classical plate theory; bi-harmonic equation; arbitrary boundary conditions

* Corresponding author. Tel.: +44 20 7040 8924.
Email address: j.r.banerjee@city.ac.uk

Nomenclature

w	transverse displacement
$h, 2a, 2b$	thickness and dimensions of the rectangular plate
ω, Ω	circular frequency and frequency parameter
E, ν, ρ, D	Young's modulus, Poisson ratio, density and bending stiffness of the plate
W, ϕ_y, ϕ_x	amplitudes of transverse displacement and bending rotations on the boundaries
V_x, V_y, M_x, M_y	amplitudes of shear forces and bending moments on the boundaries
$\tilde{\mathbf{d}}, \tilde{\mathbf{f}}$	amplitudes of boundary displacement and force vectors
$\alpha_n, \beta_n,$	wave numbers for the symmetric components of displacements
$\tilde{\alpha}_n, \tilde{\beta}_n,$	wave numbers for the antisymmetric components of displacements
$p_{1n}, p_{2n}, q_{1n}, q_{2n}$	roots of the characteristic equation
(k,j)	indicators of symmetric/antisymmetric components with $k,j \in \{0,1\}$
A_n, B_n, C_n, D_n	unknown coefficients of the general solution
$\mathbf{W}, \boldsymbol{\varphi}, \mathbf{M}, \mathbf{V}$	sequence vectors of Fourier coefficients for displacements, rotations, bending moments and shear forces at the boundaries
$\mathbf{A}, \mathbf{P}, \mathbf{Q}$	coefficient matrices in the mixed formulation
$\mathbf{d}, \mathbf{f}$	Fourier coefficients of the amplitudes of displacement and force vectors
$\mathbf{K}$	dynamic stiffness matrix
G_j	asymptotic constant in limitant analysis
j	number of eigenvalues between zero and a trial frequency
$j_0, s\{\mathbf{K}_f\}$	parameters needed in the application of Wittrick-Williams algorithm

2

1. Introduction

The free vibration analysis of plates and plate assemblies is a topic which has continually inspired researchers for well over two centuries. From an engineering perspective, the importance of this topic cannot be over emphasized, particularly for its applications in aeronautical industry where the top and bottom skins of an aircraft wing are generally idealised as plate assemblies during the structural design. Researchers who laid the foundation for the current state of the art on the subject include Chladni [1], Poisson [2], Lord Rayleigh [3], Ritz [4], Timoshenko [5] and Iguchi [6], amongst others. These early pioneers developed analytical methods, later referred to as classical methods, at a time when the finite element method (FEM) was not even invented and the computer power was almost non-existent. Then with the advent and rapid growth of powerful digital computers, the FEM emerged in the 1960s as a breakthrough in solid mechanics and it became possible to obtain approximate solutions for static and dynamic problems of structures such as beams, plates and their assemblies through the use of assumed shape functions. During this period, interest in classical methods continued and in fact was growing steadily to validate and importantly, to give due recognition and importance to the FEM and to put it on a reliable, but secure foundation. It was natural and understandable that classical methods which rely on the solution of the governing differential equations were comprehensively used at the time to validate the FEM. Logically the classical methods provided the ultimate benchmark to the solution of the plate vibration problem and thus became an indispensable aid to validate the FEM which is basically a numerical method. For a better insight into the problem, Leissa [7, 8] recognised the continuing need for the development of the classical methods and provided a comprehensive coverage of the free vibration analysis of rectangular plates. By and large his methods relied on the solution of the differential equation governing the plate motion undergoing free vibration, but they were not sufficiently general to cover all possible boundary conditions of the plate in an exact sense when arriving at the solution. Other notable contributors who used analytical approach, but applied different methods other than the FEM, are Warburton [9], Gorman [10], Azimi *et al* [11], Bhat [12], Cheung and Kong [13], and Xing and Liu [14, 15]. There are some excellent texts which elucidate the classical theories of plates [16-18].

Against the above background, it is useful to note that an elegant and powerful alternative to the FEM and classical methods in free vibration analysis exists, but relatively unknown which is notably the dynamic stiffness method (DSM). The method gives exact results like some of the classical methods, but has the added advantage of handling complex structures for which individual element stiffness matrices comprising the structure can be assembled to provide solutions for the whole structure. The basic building block in the DSM is the frequency dependent dynamic stiffness (DS) matrix of a structural element. The DS matrix is generally obtained from the exact solutions of the governing differential equations of the structural element undergoing free vibration. The solutions are essentially exact shape functions which, unlike the FEM, are not based on assumed interpolation polynomials to define the element deformation. Thus the accuracy achieved in the DSM is independent of the number of elements used in the analysis so that any number or order of natural

frequencies can be computed, even from a single structural element to any desired accuracy which of course, is impossible in the FEM or in any other approximate methods. When dissimilar elements are used in the DSM to model a complex structure, the DS elements are assembled in the usual way like the FEM, leading to an eigenvalue solution procedure for computing natural frequencies and mode shapes. In such cases, there will be no loss of accuracy, and the results from the DSM for the complex structure will still be exact. This is in sharp contrast to FEM for which the results are not exact because of the assumptions made in the shape functions.

For beam elements, the DSM is well established [19-21] and notably software based on the DSM is available [22, 23] for exact free vibration analysis of skeletal structures. For a plate element, the DSM was first developed by Wittrick and Williams [24] for plates and plate assemblies in the early seventies by using classical theory. This was a significant achievement at that time and the theory was implemented in a program called VIPASA [24]. However, their work was restricted to thin plates for which two opposite sides must be simply supported. Thus the deflection of the plate was assumed to vary sinusoidally in the longitudinal direction. In 1983, Williams and Anderson [25] made significant extension to the work of Wittrick and Williams [24] by introducing Lagrangian multipliers to deal with rigid and/or elastic point supports on the plate and they produced an enhanced computer code VICON [26]. Following this work, optimum design features were added to form a new version of the program, called VICONOPT [27]. Two decades later, Boscolo and Banerjee [28-30] extended the DS plate theory by including the important effects of shear deformation and rotatory inertia. Their investigations cover both isotropic plates [28] and composite plates [29, 30] and were based on the first-order shear deformation theory. Fazzolari *et al* took a step further to develop the dynamic stiffness theory for anisotropic plates [31] using higher order shear deformation theory. Later, Boscolo and Banerjee [32] developed DSM using sophisticated first-order layer-wise theory for the analysis of laminated composite plates. However, all these investigations were limited to simple support boundary condition of opposite sides of the plate. The DSM development for a plate with all sides free, i.e. without any restriction on boundary conditions is very difficult. The difficulty arises from the basic requirement that the development of the DS matrix of a structural element is dependent on the exact solution of its governing differential equations of motion in free vibration, see Banerjee [33]. In the case of a thin plate, the governing differential equation is essentially the well-known bi-harmonic equation which is generally not amenable to a general solution. The equation has been known for nearly two centuries, but was mainly of mathematical interest before its application to solve plate vibration problems became apparent [34]. Over the past two decades, there have been significant advances in seeking solution for the bi-harmonic equation in an engineering or elastodynamic context. Meleshko [35] and Papkov and Meleshko [36] made ground-breaking contributions to the study of the free vibration and static bending problems of rectangular plates. This was achieved by seeking the general solution of the bi-harmonic equation. However, their investigations were focused on a plate with completely free or completely clamped boundary conditions at all edges, and they did not approach the problem from a dynamic stiffness standpoint. Nevertheless, their research on an individual

plate has opened up novel, but potential possibilities and has become an important catalyst for the present research.

As stated earlier, the fundamental basis of the dynamic stiffness formulation for a rectangular plate originates from the quest for a general solution of the free vibratory motion of the plate represented by the bi-harmonic equation. This is achieved in this paper in a robust, elegant and exact manner. To this end, the proposed theory characterises any arbitrary (asymmetric) transverse displacement of the plate in a novel way by using four sub-solutions of the bi-harmonic equation. Appropriate choices are made for their representations as even and odd functions so as to include all possible solutions. This is one of the most important steps taken during the theoretical development. Once the exact solution for the bi-harmonic equation is obtained, the expressions for bending rotation, shear force and bending moment are formulated. Finally the force displacement relationship on the plate boundaries is constructed by deriving the frequency dependent dynamic stiffness matrix whilst eliminating the unknown coefficients from the general solutions of the free vibratory motion. Although the steps leading to the dynamic stiffness matrix are explained above in a simple manner, the implementation of these steps is of huge complexity as will be shown later. It should be recognised that the solutions of the bi-harmonic equation as well as the expressions for transverse displacements, rotations, shear forces and bending moments are all in series form and the number of terms to be considered in the series to achieve desired accuracy can be decided in advance and as such there is no limitation in computer implementation of the theory developed.

2. Theory

2.1. Classical plate theory (CPT) and a general outline of the dynamic stiffness development

In a right-handed Cartesian coordinate system, Fig. 1 shows a uniform rectangular plate of length $2a$, width $2b$ and thickness h, respectively. The origin 'O' is chosen at the mid-plane and centre of the plate so that the symmetry of the plate about xy, yz and zx planes is maintained. In the derivation that follows, Kirchhoff's thin-plate assumptions [5] are adopted so that the displacement of the mid-plane is uniquely described by the transverse or flexural displacement w which is a function of the x and y coordinates only, and not of the thickness coordinate z.
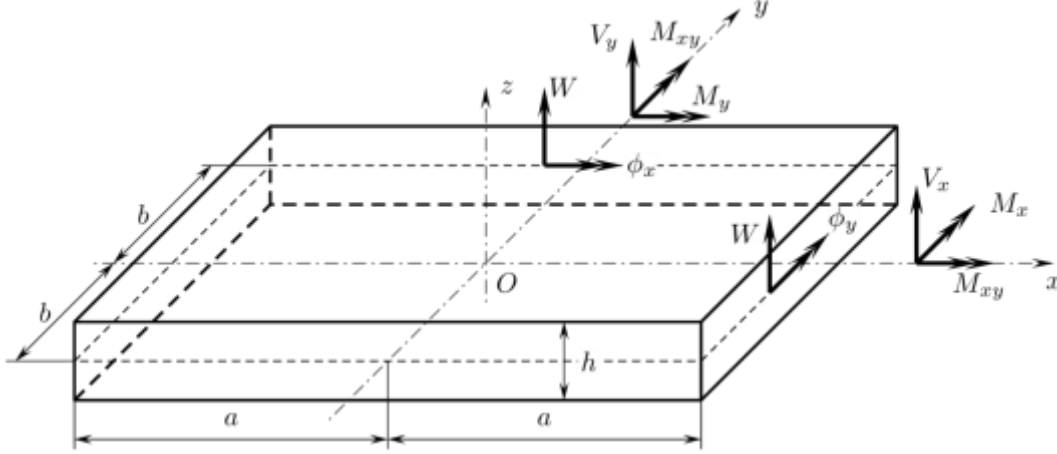
Fig. 1 Coordinate system and notations for displacements and forces for a thin plate

The governing differential equation of motion of a thin plate, as shown in Fig. 1 undergoing free vibration is well established in [7, 8] or can be derived using standard texts [16-18]. For harmonic oscillation, i.e. when $w(x, y, t) = W(x, y)e^{i\omega t}$, W being the amplitude of transverse displacement and ω the circular (or angular) frequency of oscillation, the differential equation is given by [7, 8]

$$\frac{\partial^4 W}{\partial x^4} + 2\frac{\partial^4 W}{\partial x^2 \partial y^2} + \frac{\partial^4 W}{\partial y^4} - \Omega^4 W = 0$$

(1)

where $\Omega^4 = \rho h \omega^2 / D$ is the frequency parameter, $D = Eh^3 /[12(1-\nu^2)]$ is the plate bending or flexural rigidity, E the Young's modulus, ν the Poisson ratio and ρ the density of the plate material.

The expressions for the amplitudes of the bending rotations ϕ_y and ϕ_x, the shear forces V_x and V_y and bending moments M_x and M_y per unit length in the usual notation are given by [7, 8]

$$\phi_y = -\frac{\partial W}{\partial x}; \quad \phi_x = \frac{\partial W}{\partial y};$$

(2)

$$V_x = -D\left(\frac{\partial^3 W}{\partial x^3} + (2-\nu)\frac{\partial^3 W}{\partial x \partial y^2}\right); \quad V_y = -D\left(\frac{\partial^3 W}{\partial y^3} + (2-\nu)\frac{\partial^3 W}{\partial x^2 \partial y}\right);$$

(3)

$$M_x = -D\left(\frac{\partial^2 W}{\partial x^2} + \nu\frac{\partial^2 W}{\partial y^2}\right); \quad M_y = D\left(\frac{\partial^2 W}{\partial y^2} + \nu\frac{\partial^2 W}{\partial x^2}\right);$$

(4)

It should be noted that the signs for the amplitudes of bending rotations, shear forces and bending moments in Eqs. (2)-(4) are chosen to be consistent with the sign convention shown in the right-handed coordinate system in Fig. 1.

Next, the displacement vector $\tilde{\mathbf{d}}$ comprising the amplitudes of transverse displacements and bending rotations on the four sides of the plate, and the corresponding force vector $\tilde{\mathbf{f}}$ which represents the amplitudes of shear force and bending moment, are written in the following form

$$\tilde{\mathbf{d}} = \begin{bmatrix} W(a,y) \\ \phi_y(a,y) \\ W(x,b) \\ \phi_x(x,b) \\ W(-a,y) \\ \phi_y(-a,y) \\ W(x,-b) \\ \phi_x(x,-b) \end{bmatrix} \quad \text{and} \quad \tilde{\mathbf{f}} = \begin{bmatrix} V_x(a,y) \\ M_x(a,y) \\ V_y(x,b) \\ M_y(x,b) \\ V_x(-a,y) \\ M_x(-a,y) \\ V_y(x,-b) \\ M_y(x,-b) \end{bmatrix} \tag{5}$$

It is now necessary to outline broadly the mathematical process of dynamic stiffness formulation to relate the vectors $\tilde{\mathbf{d}}$ and $\tilde{\mathbf{f}}$ of Eq. (5). A general procedure to develop the dynamic stiffness matrix of a structural element can be briefly summarized as follows

(i) Seek a closed form general solution of the governing differential equations describing the free vibratory motion of the structural element in an exact sense in terms of the unknown coefficients appearing in the general solution.

(ii) Apply general boundary conditions (BCs) in algebraic form for the amplitudes of both displacements and forces at the boundaries of the element.

(iii) Eliminate the unknown coefficients by relating the amplitudes of the harmonically varying forces to those of the corresponding displacements and thereby generating the frequency dependent dynamic stiffness matrix.

As it is well known, the closed form solution for free vibration analysis of a rectangular thin plate has been widely reported only for the special case when the opposite sides of the plate are simply supported. This is the so-called Levy solution [7, 8] which simplifies the problem drastically because it reduces the number of unknown coefficients to just four. However, for the general case when the plate is completely free to deform in any arbitrary shape, the problem becomes immensely more difficult. Therefore for the general case, it is necessary to seek the solution of the governing differential equation with sufficiently large number of unknown coefficients (which ideally extends to infinity) to satisfy any combinations of boundary conditions. Using the theory presented in this paper, such a solution can be achieved and the results can be accurate even up to machine accuracy.

2.2. General solution for free vibration of a rectangular plate

Since Eq. (1) is a linear homogeneous partial differential equation with constant coefficients, the classical

method of separation of variables allows the general solution of the type

$$W(x, y) = Ce^{px+qy}$$

(6)

where p and q are wave parameters. Substituting the above equation into Eq. (1) yields the characteristic equation

$$p^2 + q^2 = \pm\Omega^2$$

(7)

Therefore, any combination of p, q and Ω satisfying Eq. (7) represents a solution of Eq. (1). Following the work of Gorman [10], an infinite series of base solutions are sought by introducing $p_n = \pm i\alpha_n$ or $\pm i\tilde{\alpha}_n$ in the x direction, where $\alpha_n = \dfrac{\pi n}{a}$ $(n = 0, 1, 2, ...)$ and $\tilde{\alpha}_n = \dfrac{\pi}{a}(n - \dfrac{1}{2})$ $(n = 1, 2, ...)$ depending upon the symmetric or antisymmetric forms of deformation of the plate which will be explained later. An inspection of Eq. (6) indicates that the deformation in the x direction can be represented by one symmetric (even) and one anti-symmetric (odd) harmonic equations, namely

$$\left.\begin{array}{l} \dfrac{1}{2}\left(e^{i\alpha_n x} + e^{-i\alpha_n x}\right) = \cos\alpha_n x \\[2mm] \dfrac{1}{2i}\left(e^{i\alpha_n x} - e^{-i\alpha_n x}\right) = \sin\alpha_n x \end{array}\right\}$$

(8)

which applies also for $\tilde{\alpha}_n$.

Inserting $p_n = \pm i\alpha_n$ into Eq. (7) gives

$$q_n^2 = \alpha_n^2 \pm \Omega^2$$

(9)

where the roots of q_n must appear either in real or in purely imaginary pairs. In the same way, the corresponding function in y can be separated into symmetric and anti-symmetric pairs as well. A second infinite series of base solutions can be generated by letting $q_n = \pm i\beta_n$ or $\pm i\tilde{\beta}_n$ in the y direction with $\beta_n = \dfrac{\pi n}{b}$ $(n = 0, 1, 2, ...)$ or $\tilde{\beta}_n = \dfrac{\pi}{b}(n - \dfrac{1}{2})$ $(n = 1, 2, ...)$ following an analogous procedure as above. To this end, the resulting two infinite series of base solutions are added together to form the general solution W of Eq. (1). The solution can be partitioned into a sum of the four sub-solutions in each of which the function W is either even or odd. Thus letting

$$W = \sum_{k,j=0}^{1} W^{kj} = W^{00} + W^{01} + W^{10} + W^{11}$$

(10)

where the first index k denotes the symmetry relating to x and second index j denotes the symmetry relating to

y. The index '0' denotes an even function whereas '1' denotes an odd function. For example, W^{00} means W is even in both x and y whereas W^{01} means W is even in x, but odd in y and so on and so forth. Thus, the four sub-solutions describe the symmetric and anti-symmetric deformations of the plate about the mid-planes. Note that it follows from the fact that if a structure possesses a plane or planes of symmetry, any asymmetric (or un-symmetric) motion can be described by the superposition of symmetric and anti-symmetric motions. By making use of the symmetry of the structure (see Fig. 1) we can construct solution of the differential equation (1) for each of the four component cases in Eq. (10) as follows

$$
\begin{aligned}
W^{00} &= A_0 \cos \Omega y + B_0 \cosh \Omega y + C_0 \cos \Omega x + D_0 \cosh \Omega x \\
&+ \sum_{n=1}^{\infty} (A_n \cosh p_{1n} y + B_n \cosh p_{2n} y) \cos \alpha_n x + \sum_{n=1}^{\infty} (C_n \cosh q_{1n} x + D_n \cosh q_{2n} x) \cos \beta_n y
\end{aligned}
\tag{11}
$$

$$
\begin{aligned}
W^{01} &= A_0 \sin \Omega y + B_0 \sinh \Omega y + \sum_{n=1}^{\infty} (A_n \sinh p_{1n} y + B_n \sinh p_{2n} y) \cos \alpha_n x \\
&+ \sum_{n=1}^{\infty} (C_n \cosh \tilde{q}_{1n} x + D_n \cosh \tilde{q}_{2n} x) \sin \tilde{\beta}_n y
\end{aligned}
\tag{12}
$$

$$
\begin{aligned}
W^{10} &= C_0 \sin \Omega x + D_0 \sinh \Omega x + \sum_{n=1}^{\infty} (A_n \cosh \tilde{p}_{1n} y + B_n \cosh \tilde{p}_{2n} y) \sin \tilde{\alpha}_n x \\
&+ \sum_{n=1}^{\infty} (C_n \sinh q_{1n} x + D_n \sinh q_{2n} x) \cos \beta_n y
\end{aligned}
\tag{13}
$$

$$
W^{11} = \sum_{n=1}^{\infty} (A_n \sinh \tilde{p}_{1n} y + B_n \sinh \tilde{p}_{2n} y) \sin \tilde{\alpha}_n x + \sum_{n=1}^{\infty} (C_n \sinh \tilde{q}_{1n} x + D_n \sinh \tilde{q}_{2n} x) \sin \tilde{\beta}_n y
\tag{14}
$$

where

$$
\left.
\begin{aligned}
p_{1n} &= \sqrt{\alpha_n^2 - \Omega^2}; \quad p_{2n} = \sqrt{\alpha_n^2 + \Omega^2}; \quad q_{1n} = \sqrt{\beta_n^2 - \Omega^2}; \quad q_{2n} = \sqrt{\beta_n^2 + \Omega^2} \\
\tilde{p}_{1n} &= \sqrt{\tilde{\alpha}_n^2 - \Omega^2}; \quad \tilde{p}_{2n} = \sqrt{\tilde{\alpha}_n^2 + \Omega^2}; \quad \tilde{q}_{1n} = \sqrt{\tilde{\beta}_n^2 - \Omega^2}; \quad \tilde{q}_{2n} = \sqrt{\tilde{\beta}_n^2 + \Omega^2}
\end{aligned}
\right\}
\tag{15}
$$

with

$$
\left.
\begin{aligned}
\beta_n &= \pi n / b; \ \alpha_n = \pi n / a, & n = 0, 1, 2, ... \\
\tilde{\beta}_n &= \pi (n - 1/2) / b; \ \tilde{\alpha}_n = \pi (n - 1/2) / a, & n = 1, 2, ...
\end{aligned}
\right\}
\tag{16}
$$

and the unknown coefficients A_n, B_n, C_n, D_n ($n = 0, 1, 2, ...$) are different for each of the four component cases in W. Note that trigonometric and hyperbolic functions in cosine and sine exhibit even and odd characteristics which are exploited here to advantage. The symmetric (k or $j = 0$) and antisymmetric (k or $j = 1$) trigonometric functions with the first several wavenumbers α_n, β_n and $\tilde{\alpha}_n, \tilde{\beta}_n$ taken as in Eq. (16) are depicted in Fig. 2. Due to the properties of orthogonal functions, the general solution composed from Eqs. (11)-(14) can represent any prescribed transverse displacements, bending rotations/moments and shear forces on the plate

boundaries. It is quite obvious to understand this for transverse displacements because all the trigonometric functions taking the values of either -1 or 1 on the boundaries at $x=\pm a$ or $y=\pm b$ as shown in Fig. 2 where $L=a$ or b. It can be easily deduced that for any other arbitrary boundary conditions, such as the bending rotations, bending moments and shear forces defined in Eqs. (2)-(4) can be represented by the set of general solutions by looking at the second- and third-order derivatives of the solutions (11)-(14).
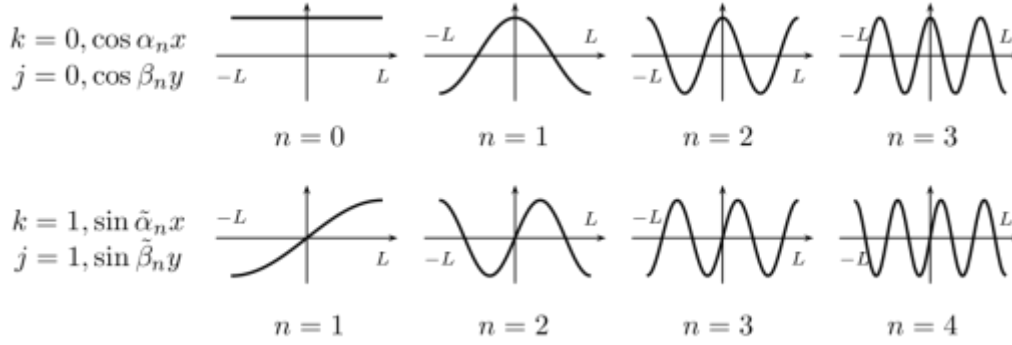

Fig. 2 The first four symmetric/antisymmetric trigonometric functions ($L=a$ or b)

Therefore the general solution given by Eq. (10) when considered as the sum of the sub-solutions given by Eqs. (11)-(14) satisfies the governing differential equation (see Eq. (1)) *a priori*. The unknown coefficients A_n, B_n, C_n, D_n need to satisfy any given boundary conditions of the plate. The fulfilling of boundary conditions leads to infinite systems of linear algebraic equations relating the Fourier coefficients of the boundary conditions (both displacements and forces). In the current work, the derived infinite system of linear algebraic equations is used to develop the dynamic stiffness matrices. We mention in passing that for a plate when all the edges are either clamped or free, the infinite systems can be solved by using limitants theory [35]. This particular aspect was investigated by Meleshko [35] and Papkov and Meleshko [36] in recent years.

The displacement and the force vectors in Eq. (5) can now be split into four symmetric and anti-symmetric components so that the sum of the four sub-vectors in each case represents the net displacement and net force acting on the boundaries of the plate. In this way one can write

$$\tilde{\mathbf{d}}^{kj} = \begin{bmatrix} W^{kj}(a,y) \\ \phi_y^{kj}(a,y) \\ W^{kj}(x,b) \\ \phi_x^{kj}(x,b) \end{bmatrix}; \quad \tilde{\mathbf{f}}^{kj} = \begin{bmatrix} V_x^{kj}(a,y) \\ M_x^{kj}(a,y) \\ V_y^{kj}(x,b) \\ M_y^{kj}(x,b) \end{bmatrix} \quad (k,j=0,1) \tag{17}$$

Now with the help of Eq. (10), the net displacement vector $\tilde{\mathbf{d}}$ and the force vector $\tilde{\mathbf{f}}$ of Eq. (5) can be written as follows:

$$
\tilde{\mathbf{d}} = \begin{bmatrix}
W^{00}(a,y)+W^{01}(a,y)+W^{10}(a,y)+W^{11}(a,y) \\
\phi_y^{00}(a,y)+\phi_y^{01}(a,y)+\phi_y^{10}(a,y)+\phi_y^{11}(a,y) \\
W^{00}(a,y)+W^{01}(a,y)-W^{10}(a,y)-W^{11}(a,y) \\
-\phi_y^{00}(a,y)-\phi_y^{01}(a,y)+\phi_y^{10}(a,y)+\phi_y^{11}(a,y) \\
W^{00}(x,b)+W^{01}(x,b)+W^{10}(x,b)+W^{11}(x,b) \\
\phi_x^{00}(x,b)+\phi_x^{01}(x,b)+\phi_x^{10}(x,b)+\phi_x^{11}(x,b) \\
W^{00}(x,b)-W^{01}(x,b)+W^{10}(x,b)-W^{11}(x,b) \\
-\phi_x^{00}(x,b)+\phi_x^{01}(x,b)-\phi_x^{10}(x,b)+\phi_x^{11}(x,b)
\end{bmatrix}
;\
\tilde{\mathbf{f}} = \begin{bmatrix}
V_x^{00}(a,y)+V_x^{01}(a,y)+V_x^{10}(a,y)+V_x^{11}(a,y) \\
M_x^{00}(a,y)+M_x^{01}(a,y)+M_x^{10}(a,y)+M_x^{11}(a,y) \\
-V_x^{00}(a,y)-V_x^{01}(a,y)+V_x^{10}(a,y)+V_x^{11}(a,y) \\
M_x^{00}(a,y)+M_x^{01}(a,y)-M_x^{10}(a,y)-M_x^{11}(a,y) \\
V_y^{00}(x,b)+V_y^{01}(x,b)+V_y^{10}(x,b)+V_y^{11}(x,b) \\
M_y^{00}(x,b)+M_y^{01}(x,b)+M_y^{10}(x,b)+M_y^{11}(x,b) \\
-V_y^{00}(x,b)+V_y^{01}(x,b)-V_y^{10}(x,b)+V_y^{11}(x,b) \\
M_y^{00}(x,b)-M_y^{01}(x,b)+M_y^{10}(x,b)-M_y^{11}(x,b)
\end{bmatrix}
\tag{18}
$$

Once the dependency between sub-vectors $\tilde{\mathbf{d}}^{kj}$ and $\tilde{\mathbf{f}}^{kj}$ is determined, which defines the dynamic stiffness matrix $\mathbf{K}^{kj}$ for each case arising from the symmetry, it becomes possible with the help of Eq. (18) to derive the overall dynamic stiffness matrix $\mathbf{K}$ for the complete plate, which relates the vectors $\tilde{\mathbf{d}}$ and $\tilde{\mathbf{f}}$.

2.3. Dynamic stiffness development

In total, four dynamic stiffness (DS) matrices $\mathbf{K}^{kj}$ should be formulated for four different symmetric and antisymmetric cases. Here for the purposes of illustration, the procedure to develop the DS matrix $\mathbf{K}^{00}$ for the component quarter plate representing the symmetry about both the *x* and the *y* axes of the whole plate is presented. The procedure for DS development for the other three cases follows similarly.

The DS matrix $\mathbf{K}^{00}$ can be formulated using two steps based on the elimination of the unknown coefficients in the general solution in Eq. (11), namely, $A_0, B_0, C_0, D_0, A_n, B_n, C_n$ and D_n. First, the unknown coefficients $A_0, B_0, C_0, D_0, A_n, B_n, C_n$ and D_n are obtained by equating the Fourier series of the boundary conditions for rotations and shear forces to the corresponding expressions obtained from the general solution and its differentiations. Secondly, the expressions of these unknowns are substituted into the boundary transverse displacements and bending moments to form an infinite system of algebraic equations which eventually leads to the DS matrix $\mathbf{K}^{00}$.

Thus as the first step, it will be shown how the unknowns $A_0, B_0, C_0, D_0, A_n, B_n, C_n$ and D_n can obtained.

Clearly the symmetric behaviours of the vectors $\tilde{\mathbf{d}}^{00}$ and $\tilde{\mathbf{f}}^{00}$ can be represented by Fourier series of the prescribed boundary conditions as follows

$$
\tilde{\mathbf{d}}^{00} = \begin{bmatrix} W_{1_0} + \sum_{n=1}^{\infty} W_{1_n} \cos \beta_n y \\[2mm] \phi_{y_0} + \sum_{n=1}^{\infty} \phi_{y_n} \cos \beta_n y \\[2mm] W_{2_0} + \sum_{n=1}^{\infty} W_{2_n} \cos \alpha_n x \\[2mm] -\phi_{x_0} - \sum_{n=1}^{\infty} \phi_{x_n} \cos \alpha_n x \end{bmatrix} ; \quad \tilde{\mathbf{f}}^{00} = -D \begin{bmatrix} V_{x_0} + \sum_{n=1}^{\infty} V_{x_n} \cos \beta_n y \\[2mm] M_{x_0} + \sum_{n=1}^{\infty} M_{x_n} \cos \beta_n y \\[2mm] V_{y_0} + \sum_{n=1}^{\infty} V_{y_n} \cos \alpha_n x \\[2mm] -M_{y_0} - \sum_{n=1}^{\infty} M_{y_n} \cos \alpha_n x \end{bmatrix} \tag{19}
$$

Alternatively, $\tilde{\mathbf{d}}^{00}$ and $\tilde{\mathbf{f}}^{00}$ can be obtained by evaluating the two-dimensional functions of Eq. (17) (all derived from general solution Eq. (11)) on the plate boundaries. From the general solution for displacement W^{00} (see Eq. (11)), the bending rotations ϕ_y^{00}, ϕ_x^{00}, the shear forces V_x^{00}, V_y^{00} and the bending moments M_x^{00}, M_y^{00} can be obtained with the help of Eqs. (2)-(4) and they are expressed as follows:

$$
\phi_y^{00}(x,y) = C_0 \Omega \sin \Omega x - D_0 \Omega \sinh \Omega x + \sum_{n=1}^{\infty} (A_n \cosh p_{1n} y + B_n \cosh p_{2n} y) \alpha_n \sin \alpha_n x
$$
$$
- \sum_{n=1}^{\infty} (C_n q_{1n} \sinh q_{1n} x + D_n q_{2n} \sinh q_{2n} x) \cos \beta_n y. \tag{20}
$$

$$
\phi_x^{00}(x,y) = -A_0 \Omega \sin \Omega y + B_0 \Omega \sinh \Omega y + \sum_{n=1}^{\infty} (A_n p_{1n} \sinh p_{1n} y + B_n p_{2n} \sinh p_{2n} y) \cos \alpha_n x
$$
$$
- \sum_{n=1}^{\infty} (C_n \cosh q_{1n} x + D_n \cosh q_{2n} x) \beta_n \sin \beta_n y. \tag{21}
$$

$$
-V_x^{00}(x,y)/D = C_0 \Omega^3 \sin \Omega x + D_0 \Omega^3 \sinh \Omega x
$$
$$
+ \sum_{n=1}^{\infty} (A_n (\alpha_n^2 - (2-v) p_{1n}^2) \cosh p_{1n} y + B_n (\alpha_n^2 - (2-v) p_{2n}^2) \cosh p_{2n} y) \alpha_n \sin \alpha_n x
$$
$$
+ \sum_{n=1}^{\infty} (C_n q_{1n} (q_{1n}^2 - (2-v) \beta_n^2) \sinh q_{1n} x + D_n q_{2n} (q_{2n}^2 - (2-v) \beta_n^2) \sinh q_{2n} x) \cos \beta_n y. \tag{22}
$$

$$
-V_y^{00}(x,y)/D = A_0 \Omega^3 \sin \Omega y + B_0 \Omega^3 \sinh \Omega y
$$
$$
+ \sum_{n=1}^{\infty} (A_n p_{1n} (p_{1n}^2 - (2-v) \alpha_n^2) \sinh p_{1n} y + B_n p_{2n} (p_{2n}^2 - (2-v) \alpha_n^2) \sinh p_{2n} y) \cos \alpha_n x
$$
$$
+ \sum_{n=1}^{\infty} (C_n (\beta_n^2 - (2-v) q_{1n}^2) \cosh q_{1n} x + D_n (\beta_n^2 - (2-v) q_{2n}^2) \cosh q_{2n} x) \beta_n \sin \beta_n y. \tag{23}
$$

$$-M_x^{00}(x,y)/D = -A_0 \nu \Omega^2 \cos \Omega y + B_0 \nu \Omega^2 \cosh \Omega y - C_0 \Omega^2 \cos \Omega x + D_0 \Omega^2 \cosh \Omega x$$

$$+ \sum_{n=1}^{\infty} (A_n (\nu p_{1n}^2 - \alpha_n^2) \cosh p_{1n} y + B_n (\nu p_{2n}^2 - \alpha_n^2) \cosh p_{2n} y) \cos \alpha_n x$$

$$+ \sum_{n=1}^{\infty} (C_n (q_{1n}^2 - \nu \beta_n^2) \cosh q_{1n} x + D_n (q_{2n}^2 - \nu \beta_n^2) \cosh q_{2n} x) \cos \beta_n y. \tag{24}$$

$$M_y^{00}(x,y)/D = -A_0 \Omega^2 \cos \Omega y + B_0 \Omega^2 \cosh \Omega y - C_0 \nu \Omega^2 \cos \Omega x + D_0 \nu \Omega^2 \cosh \Omega x$$

$$+ \sum_{n=1}^{\infty} (A_n (p_{1n}^2 - \nu \alpha_n^2) \cosh p_{1n} y + B_n (p_{2n}^2 - \nu \alpha_n^2) \cosh p_{2n} y) \cos \alpha_n x$$

$$+ \sum_{n=1}^{\infty} (C_n (\nu q_{1n}^2 - \beta_n^2) \cosh q_{1n} x + D_n (\nu q_{2n}^2 - \beta_n^2) \cosh q_{2n} x) \cos \beta_n y. \tag{25}$$

A close inspection on Eqs (20)-(25) reveals that the expressions with odd order derivatives of W^{00} (rotation and shear forces) are of simpler forms on the boundaries which can be used to determine all of the unknown coefficients in terms of the Fourier coefficients of the boundary rotations and shear forces only. For example, in Eqs. (20) and (22), the terms including $\sin \alpha_n x$ vanish on the boundary at $x = a$ since $\sin \alpha_n a = 0$. Similarly, the conditions $\sin \beta_n y = 0$ in Eqs. (21) and (23) on the boundary at $y = b$ will be valid. Based on this observation, the following equalities can be obtained by equating Eqs. (20)-(23) on the boundaries to the corresponding terms of Fourier series in Eq. (19).

$$\phi_y^{00}(a,y) = C_0 \Omega \sin \Omega a - D_0 \Omega \sinh \Omega a - \sum_{n=1}^{\infty} (C_n q_{1n} \sinh q_{1n} a + D_n q_{2n} \sinh q_{2n} a) \cos \beta_n y$$

$$= \phi_{y_0} + \sum_{n=1}^{\infty} \phi_{y_n} \cos \beta_n y, \tag{26}$$

$$V_x^{00}(a,y) = -D \Big(C_0 \Omega^3 \sin \Omega a + D_0 \Omega^3 \sinh \Omega a + \sum_{n=1}^{\infty} (C_n q_{1n} (q_{1n}^2 - (2-\nu)\beta_n^2) \sinh q_{1n} a$$

$$+ D_n q_{2n} (q_{2n}^2 - (2-\nu)\beta_n^2) \sinh q_{2n} a) \cos \beta_n y \Big) = -D \Big(V_{x_0} + \sum_{n=1}^{\infty} V_{x_n} \cos \beta_n y \Big), \tag{27}$$

$$\phi_x^{00}(x,b) = -A_0 \Omega \sin \Omega b + B_0 \Omega \sinh \Omega b + \sum_{n=1}^{\infty} (A_n p_{1n} \sinh p_{1n} b + B_n p_{2n} \sinh p_{2n} b) \cos \alpha_n x$$

$$= -\phi_{x_0} - \sum_{n=1}^{\infty} \phi_{x_n} \cos \alpha_n x, \tag{28}$$

$$V_y^{00}(x,b) = -D \Big(A_0 \Omega^3 \sin \Omega b + B_0 \Omega^3 \sinh \Omega b + \sum_{n=1}^{\infty} (A_n p_{1n} (p_{1n}^2 - (2-\nu)\alpha_n^2) \sinh p_{1n} b$$

$$+ B_n p_{2n} (p_{2n}^2 - (2-\nu)\alpha_n^2) \sinh p_{2n} b) \cos \alpha_n x \Big) = -D \Big(V_{y_0} + \sum_{n=1}^{\infty} V_{y_n} \cos \alpha_n x \Big). \tag{29}$$

13

The Eqs. (26) and (27) lead to the following systems of equations

$$\left.\begin{array}{l} C_0 \sin \Omega a - D_0 \sinh \Omega a = \phi_{y_0} / \Omega \\ C_0 \sin \Omega a + D_0 \sinh \Omega a = V_{x_0} / \Omega^3 \end{array}\right\} \tag{30}$$

$$\left.\begin{array}{l} C_n q_{1n} \sinh q_{1n} a + D_n q_{2n} \sinh q_{2n} a = -\phi_{y_n} \\ C_n q_{1n} (q_{1n}^2 - (2-v)\beta_n^2) \sinh q_{1n} a + D_n q_{2n} (q_{2n}^2 - (2-v)\beta_n^2) \sinh q_{2n} a = V_{x_n} \end{array}\right\} \tag{31}$$

Similarly, Eqs. (28) and (29) yield

$$\left.\begin{array}{l} A_0 \sin \Omega b - B_0 \sinh \Omega b = \phi_{x_0} / \Omega \\ A_0 \sin \Omega b + B_0 \sinh \Omega b = V_{y_0} / \Omega^3 \end{array}\right\} \tag{32}$$

$$\left.\begin{array}{l} A_n p_{1n} \sinh p_{1n} b + B_n p_{2n} \sinh p_{2n} b = -\phi_{x_n} \\ A_n p_{1n} (p_{1n}^2 - (2-v)\alpha_n^2) \sinh p_{1n} b + B_n p_{2n} (p_{2n}^2 - (2-v)\alpha_n^2) \sinh p_{2n} b = V_{y_n} \end{array}\right\} \tag{33}$$

The solutions of system of Eqs. (30)-(33) can be written as:

$$A_0 = \frac{V_{y_0} + \Omega^2 \phi_{x_0}}{2\Omega^3 \sin \Omega b} ; \quad B_0 = \frac{V_{y0} - \Omega^2 \phi_{x0}}{2\Omega^3 \sinh \Omega b} ; \quad C_0 = \frac{V_{x_0} + \Omega^2 \phi_{y_0}}{2\Omega^3 \sin \Omega a} ; \quad D_0 = \frac{V_{x_0} - \Omega^2 \phi_{y_0}}{2\Omega^3 \sinh \Omega a} ; \tag{34}$$

$$\left.\begin{array}{l} A_n = -\dfrac{V_{y_n} + (p_{2n}^2 - (2-v)\alpha_n^2)\phi_{x_n}}{2\Omega^2 p_{1n} \sinh p_{1n} b} ; \quad B_n = \dfrac{V_{y_n} + (p_{1n}^2 - (2-v)\alpha_n^2)\phi_{x_n}}{2\Omega^2 p_{2n} \sinh p_{2n} b} \\[4mm] C_n = -\dfrac{V_{x_n} + (q_{2n}^2 - (2-v)\beta_n^2)\phi_{y_n}}{2\Omega^2 q_{1n} \sinh q_{1n} a} ; \quad D_n = \dfrac{V_{x_n} + (q_{1n}^2 - (2-v)\beta_n^2)\phi_{y_n}}{2\Omega^2 q_{2n} \sinh q_{2n} a} \end{array}\right\} \tag{35}$$

Thus all unknown coefficients are now expressed by Fourier coefficients for boundary rotations and shear forces.

In the next step, an infinite system of linear algebraic equation is obtained by substituting the already determined unknowns $A_0, B_0, C_0, D_0, A_n, B_n, C_n$ and D_n given by Eqs. (34) and (35) into the boundary conditions for transverse displacements and bending moments in Eqs. (11), (24) and (25) so that the infinite system relates the Fourier coefficients of the boundary displacements and forces. The derivations were complex but carried out both manually as well as by using symbolic computation package Mathematica and they were checked against each other. The expressions are recorded in Appendices **A-C**. Then the dynamic stiffness matrices are formulated from this infinite system by using some further steps of matrix manipulation. Note that the following matrix reorganisations are applicable only to the doubly-symmetric component case ($k=j=0$), but for the remaining three component cases the procedure is analogous. The infinite system of equations (A.5)-(A.12) can now be rewritten in the following matrix form:

$$\left.\begin{array}{r} \mathbf{A}^{clamped}\mathbf{V} + \mathbf{W} + \mathbf{A}^{mix1}\boldsymbol{\varphi} = \mathbf{0} \\ \mathbf{A}^{free}\boldsymbol{\varphi} + \mathbf{M} + \mathbf{A}^{mix2}\mathbf{V} = \mathbf{0} \end{array}\right\} \tag{36}$$

where the sequences of Fourier coefficients for boundary displacements, rotations, bending moments and shear forces are

$$\left.\begin{array}{l} \mathbf{W} = \{W_{1_0}, W_{2_0}, ..., W_{1m}, W_{2_m}, ...\}^T \\ \boldsymbol{\varphi} = \{\phi_{y_0}, \phi_{x_0}, ..., \phi_{y_m}, \phi_{x_m}, ...\}^T \\ \mathbf{M} = \{M_{x_0}, M_{y_0}, ..., M_{x_m}, M_{y_m}, ...\}^T \\ \mathbf{V} = \{V_{x_0}, V_{y_0}, ..., V_{x_m}, V_{y_m}, ...\}^T \end{array}\right\} \tag{37}$$

and the frequency dependent elements of the infinite order matrices $\mathbf{A}^{clamped}$, $\mathbf{A}^{free}$, $\mathbf{A}^{mix1}$, $\mathbf{A}^{mix2}$ of Eq. (36) can be easily obtained from the system of Eqs. (A.5)-(A.12). The elements are given in explicit algebraic form in Appendix **D**.

For a plate with free boundary condition on all sides, one requires $\mathbf{M} = \mathbf{V} = \mathbf{0}$ in Eq. (36) which gives

$$\left.\begin{array}{r} \mathbf{W} + \mathbf{A}^{mix1}\boldsymbol{\varphi} = \mathbf{0} \\ \mathbf{A}^{free}\boldsymbol{\varphi} = \mathbf{0} \end{array}\right\} \tag{38}$$

Therefore natural frequencies for a plate with all sides free can be obtained from the equation

$$\det\begin{bmatrix} \mathbf{I} & \mathbf{A}^{mix1} \\ \mathbf{0} & \mathbf{A}^{free} \end{bmatrix} = \det \mathbf{A}^{free} = 0 \tag{39}$$

In an analogous way, the natural frequencies for an all-round clamped plate can be obtained by substituting $\mathbf{W} = \boldsymbol{\varphi} = \mathbf{0}$ in Eq. (36) leading to the following determinant to give the frequency equation

$$\det \mathbf{A}^{clamped} = 0 \tag{40}$$

The displacement sequences $\mathbf{W}$ and $\boldsymbol{\varphi}$ can now be expressed with the help of Eq. (36) as

$$\left.\begin{array}{r} \mathbf{W} = \mathbf{P}^{11}\mathbf{V} + \mathbf{P}^{12}\mathbf{M} \\ \boldsymbol{\varphi} = \mathbf{P}^{21}\mathbf{V} + \mathbf{P}^{22}\mathbf{M} \end{array}\right\} \tag{41}$$

where

$$\left.\begin{array}{ll} \mathbf{P}^{11} = \mathbf{A}^{mix1}(\mathbf{A}^{free})^{-1}\mathbf{A}^{mix2} - \mathbf{A}^{clamped}; & \mathbf{P}^{12} = \mathbf{A}^{mix1}(\mathbf{A}^{free})^{-1} \\ \mathbf{P}^{21} = -(\mathbf{A}^{free})^{-1}\mathbf{A}^{mix2}; & \mathbf{P}^{22} = -(\mathbf{A}^{free})^{-1} \end{array}\right\} \tag{42}$$

This approach is based on the inverse of matrix $(\mathbf{A}^{free})^{-1}$ and it allows the construction of the inverse of the dynamic stiffness matrix in the following manner

$$\left(\mathbf{K}^{00}\right)_{mn}^{-1} = \begin{bmatrix} \mathbf{P}_{mn}^{11} & \mathbf{P}_{mn}^{12} \\ \mathbf{P}_{mn}^{21} & \mathbf{P}_{mn}^{22} \end{bmatrix}, \qquad (m, n = 1, 2, \ldots) \tag{43}$$

Here the dynamic stiffness matrix $\mathbf{K}^{00}$ relates $\mathbf{f}^{00}$ and $\mathbf{d}^{00}$

$$\mathbf{f}^{00} = \mathbf{K}^{00}\mathbf{d}^{00} \tag{44}$$

in which

$$\mathbf{f}^{00} = [\mathbf{V}, \mathbf{M}]^T, \quad \mathbf{d}^{00} = [\mathbf{W}, \boldsymbol{\varphi}]^T \tag{45}$$

The vectors $\mathbf{V}, \mathbf{M}, \mathbf{W}, \boldsymbol{\varphi}$ in Eq. (45) have already been defined earlier in Eq. (37). Clearly that $\mathbf{f}^{00}$ and $\mathbf{d}^{00}$ are the Fourier coefficient vectors of the boundary force and displacement vectors $\tilde{\mathbf{f}}^{00}$ and $\tilde{\mathbf{d}}^{00}$ respectively.

The accuracy of the dynamic stiffness elements of Eq. (43) will greatly depend on the accuracy of the inverse of the matrix $\mathbf{A}^{free}$. This matrix corresponds to quasi-regular operator in space of limited sequences ℓ_∞ that makes an accurate inverse of the matrix possible on the basis of the method of reduction. The main advantage of such an approach is the provision of obtaining practically almost exact inverse of the matrix $\mathbf{A}^{free}$. If elements of the matrix are defined as $(\mathbf{A}^{free})^{-1} = \{z_{mn}\}_{m,n=0}^{\infty}$ (starting index used is 0 for convenience), then the following matrix equality must be satisfied

$$\mathbf{A}^{free}(\mathbf{A}^{free})^{-1} - \mathbf{I} = \mathbf{O} \tag{46}$$

where $\mathbf{I}$ and $\mathbf{O}$ are respectively the identity matrix and null matrix of the same order as $\mathbf{A}^{free}$.

Equation (46) leads to the following infinite system for each column of matrix $\{z_{m,j}\}_{m=0}^{\infty}$ $(j = 0, 1, 2 \ldots)$ as

$$\frac{\Omega(\cot\Omega a + \coth\Omega a)}{2} z_{0j} + \frac{\nu}{b} z_{1j} = \frac{\nu\Omega^4}{b} \sum_{n=1}^{\infty} \frac{(-1)^n}{p_{1n}^2 p_{2n}^2} z_{2n+1,j} + \delta_{j0} \tag{47}$$

$$\frac{\nu}{a} z_{0j} + \frac{\Omega(\cot\Omega b + \coth\Omega b)}{2} z_{1j} = \frac{\nu\Omega^4}{a} \sum_{n=1}^{\infty} \frac{(-1)^n}{q_{1n}^2 q_{2n}^2} z_{2n,j} + \delta_{j1} \tag{48}$$

$$(-1)^m z_{2m,j} = \frac{4\nu\Omega^6}{b\Delta_{5m}q_{1m}^2 q_{2m}^2} z_{1j} + \frac{4\Omega^2}{b\Delta_{5m}} \sum_{n=1}^{\infty} \frac{(1-\nu)^2\beta_m^2\alpha_n^2 + \nu\Omega^4}{(\alpha_n^2 + q_{1m}^2)(\alpha_n^2 + q_{2m}^2)} (-1)^n z_{2n+1,j} + \frac{2\Omega^2(-1)^m\delta_{j,2m}}{\Delta_{5m}} \tag{49}$$

16

$$(-1)^m z_{2m+1,j} = \frac{4\nu\Omega^6}{a\Delta_{7m}p_{1m}^2 p_{2m}^2} z_{0j} + \frac{4\Omega^2}{a\Delta_{7m}} \sum_{n=1}^{\infty} \frac{(1-\nu)^2 \beta_n^2 \alpha_m^2 + \nu\Omega^4}{(\beta_n^2 + p_{1m}^2)(\beta_n^2 + p_{2m}^2)} (-1)^n z_{2n,j} + \frac{2\Omega^2(-1)^m \delta_{j,2m+1}}{\Delta_{7m}}$$

(50)

where $m = 0, 1, 2, \ldots, N$.

Following the methodology outlined by Meleshko [35] one can now evaluate the coefficients of the system of Eqs. (47)-(50) by using the following limits

$$\lim_{m\to\infty} \frac{4\Omega^2}{b\Delta_{5m}} \sum_{n=1}^{\infty} \frac{(1-\nu)^2 \beta_m^2 \alpha_n^2 + \nu\Omega^4}{(\alpha_n^2 + q_{1m}^2)(\alpha_n^2 + q_{2m}^2)} = \lim_{m\to\infty} \frac{4\Omega^2}{a\Delta_{7m}} \sum_{n=1}^{\infty} \frac{(1-\nu)^2 \beta_n^2 \alpha_m^2 + \nu\Omega^4}{(\beta_n^2 + p_{1m}^2)(\beta_n^2 + p_{2m}^2)} = \frac{1-\nu}{3+\nu} < 1$$

(51)

Clearly the infinite system of Eqs. (47)-(50) is *quasi-regular*. Thus there exists some number N_R such that the sum of the off-diagonal elements of each row m ($m > N_R$) of the infinite coefficient matrix of the right-hand side of Eqs. (47)-(50) is less than the corresponding diagonal element which will always have a positive value. According to the general theory of Kantorovich and Krylov [39], the system of Eqs (47)-(50) will have unique solution in the space of bounded sequences ℓ_∞ for frequencies which are different from natural frequencies.

Using the limitants theory which was originally proposed by Koialovich [37] and generalised by Papkov [38], one can prove that the bounded solution of this system can be described by asymptotic formula ($m \to \infty$) as follows:

$$z_{2m,j} = \frac{(-1)^m bG_j}{\beta_m^{2+\lambda}} \quad z_{2m+1,j} = \frac{(-1)^m aG_j}{\alpha_m^{2+\lambda}}$$

(52)

where G_j is some constant and $\lambda \in (0, 1)$ is a root of the following transcendental equation

$$\frac{(1-\nu)(1+\lambda)}{3+\nu} = \cos\frac{\pi\lambda}{2}$$

(53)

Based on the knowledge of the asymptotic behavior described by Eq. (52) it is now possible to use the method of improved reduction [35, 36] for constructing the matrix $(\mathbf{A}^{free})^{-1}$. For each infinite column of the resultant matrix on the left hand side of Eqs. (47)-(50), one can determine $2N+2$ unknowns $z_{0j}, z_{1j}, \ldots, z_{2N,j}, z_{2N+1,j}$ (i.e., the first $2N+2$ elements of the *jth* column of matrix $(\mathbf{A}^{free})^{-1}$) and one asymptotic constant G_j, which leads to the following reduced system with $2N + 3$ equations to provide the solutions

$$\frac{\Omega(\cot\Omega a + \coth\Omega a)}{2} z_{0j} + \frac{\nu}{b} z_{1j} = \frac{\nu\Omega^4}{b} \sum_{n=1}^{N} \frac{(-1)^n}{p_{1n}^2 p_{2n}^2} z_{2n+1,j} + \frac{\nu\Omega^4 aG_j}{b} \sum_{n=N+1}^{\infty} \frac{1}{\alpha_n^{2+\lambda} p_{1n}^2 p_{2n}^2} + \delta_{j0}$$

(54)

17

$$\frac{v}{a}z_{0j} + \frac{\Omega(\cot\Omega b + \coth\Omega b)}{2}z_{1j} = \frac{v\Omega^4}{a}\sum_{n=1}^{N}\frac{(-1)^n}{q_{1n}^2 q_{2n}^2}z_{2n,j} + \frac{v\Omega^4 bG_j}{a}\sum_{n=N+1}^{\infty}\frac{1}{\beta_n^{2+\lambda}q_{1n}^2 q_{2n}^2} + \delta_{j1} \tag{55}$$

$$(-1)^m z_{2m,j} = \frac{4v\Omega^6}{b\Delta_{5m}q_{1m}^2 q_{2m}^2}z_{1j} + \frac{4\Omega^2}{b\Delta_{5m}}\sum_{n=1}^{N}\frac{((1-v)^2\beta_m^2\alpha_n^2 + v\Omega^4)}{(\alpha_n^2 + q_{1m}^2)(\alpha_n^2 + q_{2m}^2)}(-1)^n z_{2n+1,j}$$
$$+ \frac{4\Omega^2 aG_j}{b\Delta_{5m}}\sum_{n=N+1}^{\infty}\frac{((1-v)^2\beta_m^2\alpha_n^2 + v\Omega^4)}{(\alpha_n^2 + q_{1m}^2)(\alpha_n^2 + q_{2m}^2)\alpha_n^{2+\lambda}} + \frac{2\Omega^2(-1)^m\delta_{j,2m}}{\Delta_{5m}} \tag{56}$$

$$(-1)^m z_{2m+1,j} = \frac{4v\Omega^6}{a\Delta_{7m}p_{1m}^2 p_{2m}^2}z_{0j} + \frac{4\Omega^2}{a\Delta_{7m}}\sum_{n=1}^{N}\frac{(1-v)^2\beta_n^2\alpha_m^2 + v\Omega^4}{(\beta_n^2 + p_{1m}^2)(\beta_n^2 + p_{2m}^2)}(-1)^n z_{2n,j}$$
$$+ \frac{4\Omega^2 bG_j}{a\Delta_{7m}}\sum_{n=N+1}^{\infty}\frac{(1-v)^2\beta_n^2\alpha_m^2 + v\Omega^4}{(\beta_n^2 + p_{1m}^2)(\beta_n^2 + p_{2m}^2)\beta_n^{2+\lambda}} + \frac{2\Omega^2(-1)^m\delta_{j,2m+1}}{\Delta_{7m}} \tag{57}$$

$$G_j = \frac{(-1)^N}{2}\left(\frac{z_{2N,j}\beta_N^{2+\lambda}}{b} + \frac{z_{2N+1,j}\alpha_N^{2+\lambda}}{a}\right) \tag{58}$$

where $m = 0, 1, 2,\ldots, N$.

Obviously, if a similar system is analysed in terms of the rows of matrix $(\mathbf{A}^{free})^{-1}$ from Eq. (46), the same results can be obtained. Therefore the solution of the system of Eqs. (47)-(50) enables the inversion of the matrix $\mathbf{A}^{free}$ with vastly improved accuracy. Furthermore, it should be recognised that the values of asymptotic formula for all elements have been successfully achieved.

An alternative way to constructe the dynamic stiffness matrix would be to seek expressions for the force sequences $\mathbf{V}$ and $\mathbf{M}$ instead. This is based on the system of Eqs. (36) to give

$$\left.\begin{array}{l}\mathbf{V} = \mathbf{Q}^{11}\mathbf{W} + \mathbf{Q}^{12}\boldsymbol{\varphi} \\ \mathbf{M} = \mathbf{Q}^{21}\mathbf{W} + \mathbf{Q}^{22}\boldsymbol{\varphi}\end{array}\right\} \tag{59}$$

where

$$\left.\begin{array}{ll}\mathbf{Q}^{11} = -(\mathbf{A}^{clamped})^{-1}; & \mathbf{Q}^{12} = -(\mathbf{A}^{clamped})^{-1}\mathbf{A}^{mix1} \\ \mathbf{Q}^{21} = \mathbf{A}^{mix2}(\mathbf{A}^{clamped})^{-1}; & \mathbf{Q}^{22} = \mathbf{A}^{mix2}(\mathbf{A}^{clamped})^{-1}\mathbf{A}^{mix1} - \mathbf{A}^{free}\end{array}\right\} \tag{60}$$

The 2×2 block dynamic stiffness matrix for the symmetric case can thus be represented by

$$\mathbf{K}_{mn}^{00} = \begin{bmatrix}\mathbf{Q}_{mn}^{11} & \mathbf{Q}_{mn}^{12} \\ \mathbf{Q}_{mn}^{21} & \mathbf{Q}_{mn}^{22}\end{bmatrix} \quad (m, n = 1,2,\ldots) \tag{61}$$

However, the asymptotic formula for obtaining $(\mathbf{A}^{clamped})^{-1}$ is extremely difficult and therefore, it is preferable

to derive the dynamic stiffness matrix by using Eq. (43).

By using Eq. (43), one can obtain the stiffness matrix $\mathbf{K}^{00}$ and similarly, $\mathbf{K}^{kj}$ for the three other component cases can be formulated. Relevant expressions for the remaining three cases other than $\mathbf{K}^{00}$ are recorded in Appendix **C**. Finally, with the help of Eq. (18), the overall DS matrix $\mathbf{K}$ of the entire plate can be constructed from the four component cases $\mathbf{K}^{kj}$. Thus, the final DS matrix $\mathbf{K}$ relating $\mathbf{d}$ and $\mathbf{f}$ is given in the form

$$\mathbf{f} = \mathbf{Kd} \tag{62}$$

where the vectors $\mathbf{f}$ and $\mathbf{d}$ are the Fourier coefficient vectors of the arbitrarily prescribed boundary force and displacement vectors $\tilde{\mathbf{f}}$ and $\tilde{\mathbf{d}}$ respectively.

It is often instructive to partition the overall dynamics stiffness matrix $\mathbf{K}$ according to commonly used specified boundary conditions of the plate. Suppose that the displacement vector $\mathbf{d}$ can be partitioned into two sub-vectors $\mathbf{d}_a$ and $\mathbf{d}_b$ such that the displacement sub-vector $\mathbf{d}_b$ (which corresponds to $\mathbf{f}_b$) and the force sub-vector $\mathbf{f}_a$ (which corresponds to $\mathbf{d}_a$) are known from the prescribed boundary conditions. Then Eq. (62) can be recast in the following form

$$\begin{bmatrix} \mathbf{K}_{aa} & \mathbf{K}_{ab} \\ \mathbf{K}_{ba} & \mathbf{K}_{bb} \end{bmatrix} \begin{bmatrix} \mathbf{d}_a \\ \mathbf{d}_b \end{bmatrix} = \begin{bmatrix} \mathbf{f}_a \\ \mathbf{f}_b \end{bmatrix} \tag{63}$$

where $\mathbf{K}_{ab} = \mathbf{K}_{ba}^T$. For many practical applications of free vibration analysis, $\mathbf{f}_a$ and $\mathbf{d}_b$ are taken as zero vectors. In such cases, Eq. (63) is reduced to

$$\mathbf{K}_{aa}\mathbf{d}_a = \mathbf{0} \tag{64}$$

Thus the natural frequencies can be computed through searching for the zeros of the determinant of the above reduced DS matrix $\mathbf{K}_{aa}$. Note that the case of a fully clamped plate cannot be accommodated in this procedure, but the problem for this case can be solved using the determinant of Eq. (40). Any arbitrarily prescribed mixed boundary conditions such as line and/or point supports on the boundaries can be represented by the Fourier coefficient vectors $\mathbf{d}$ and $\mathbf{f}$ through Fourier transforms. In particular, for constraints involving point supports, an alternative approach incorporating Lagrangian multipliers can be used [25]. Application of such point constraints using Lagrangian multipliers is beyond the scope of the present paper, but provides scope for future research. Natural frequencies and mode shapes computation follows from an adapted application of the Wittrick-Williams algorithm [40] which has been explained in some detail in Appendix **E**. For interested readers, the complete procedure of the dynamic stiffness development and its implementation is
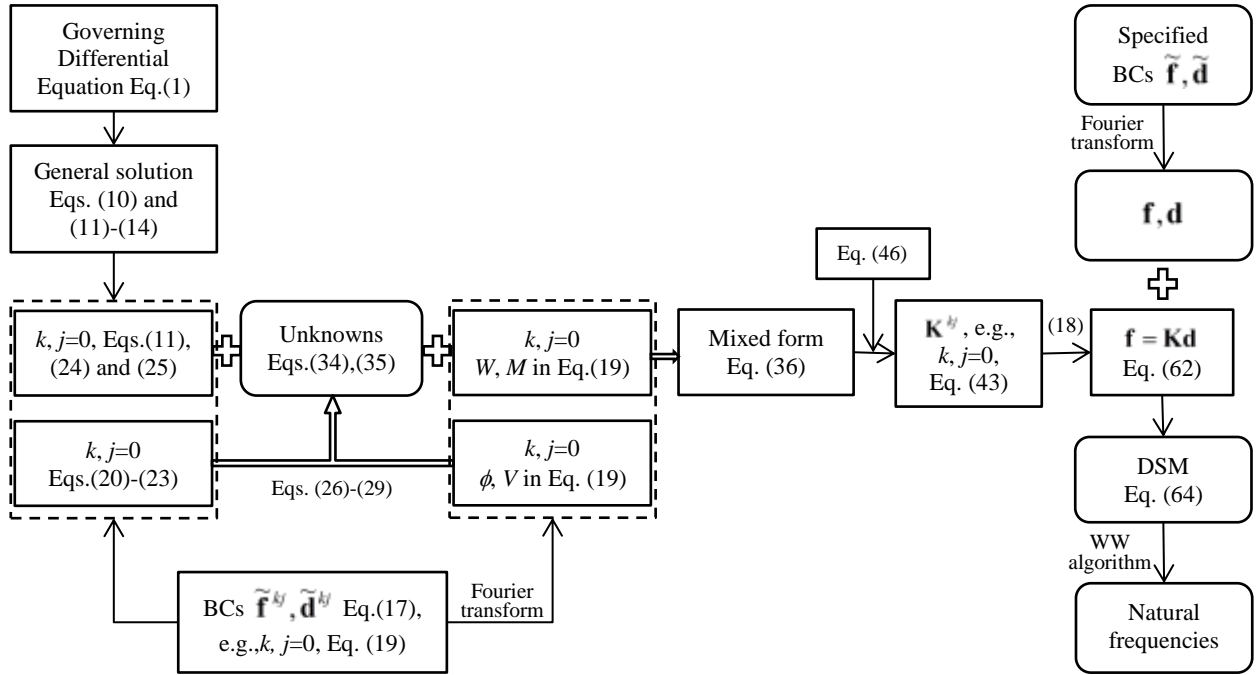
illustrated in Fig. 3.

Fig. 3 Flowchart showing the procedure for the DSM development and its implementation.

3. Results and discussion

The theory developed above has been implemented in a MATLAB program to compute the natural frequencies and mode shapes of rectangular plates with different boundary conditions. The accuracy and convergence of the results using the current method are confirmed first, which was aided by published results.

First the results for a square (a/b=1) and then for a rectangular (a/b=2) plate are computed for three types of boundary conditions. These are: (i) free all-around edges (F-F-F-F), (ii) all-around clamped edges (C-C-C-C), and (iii) opposite edges are clamped and free (C-F-C-F), respectively. It is worth emphasising that for all these three cases, either symmetric or anti-symmetric displacement and force boundary conditions with respect to x and y axes are clearly apparent. Therefore, it is expected that the corresponding mode shapes will be either symmetric or antisymmetric. That is to say, the mode shapes can be represented by one of the four sub-solutions of the general solution given in Eq. (10). If the set of boundary conditions on the four edges is asymmetric (neither symmetric nor antisymmetric), the corresponding mode shapes will be naturally asymmetric.

The first ten natural frequencies of a completely free (F-F-F-F) square plate (a/b=1, v=0.3) have been computed by the proposed DSM theory and are shown in Table 1. This particular example is relevant to the historic work by Chladni [1] who was the first to attempt the problem. In order to check the convergence of the current method, the dimensionless natural frequencies $\Omega = \sqrt[4]{\rho h \omega^2 / D}$ have been computed for two

different values of *N* where the infinite series is truncated at a given value, e.g., *n=N* in the reduction, see Eqs. (54)-(58) and the matrices in Appendix **D**. For the first ten natural frequencies, *N*=4 leads to results with satisfactory accuracy for all practical purposes, and the results with *N*=10 give accuracy up to six significant figures. Table 1 also shows excellent agreement between the results from the present theory with those obtained by the analytical method proposed by Papkov and Meleshko [36] who did not use the dynamic stiffness method, but made use of the regularity analysis of the infinite system of algebraic equations. Clearly, the use of the current approach offers the advantage to achieve any desired accuracy. Representative mode shapes are shown in Fig. 4. These are some of the typical Chladni figures for a square plate [1]. The symmetry of the mode shapes are indicated in the second column of Table 1, where the notation (*k,j*) corresponds to the '*kj*' notation defined in Eq. (10). The symmetric/anti-symmetric properties of the first ten mode shapes agree with those reported in the literature [1, 4, 7, 36]. The sixth and tenth mode shapes, illustrated in Figs. 2 (a) and (d) respectively, are doubly symmetric whereas the seventh mode shape (Fig. 4(b)) is doubly antisymmetric. By contrast, the ninth mode Figs. 2 (c) is symmetric in one direction and antisymmetric in the other direction, namely, symmetric in *x* and antisymmetric in *y*, or symmetric in *y* and antisymmetric in *x* (the two natural frequencies should be the same because it is a square plate). For consistency and ease of comparison, the natural frequency parameter with another dimensionless quantity $\lambda = 4\Omega^2$ for the same problem as above are compared with the classical solutions of Leissa [7] who used Rayleigh-Ritz method, see Table 2. It can be seen that the DSM results are in good agreement with those of the Rayleigh-Ritz method, but of course, the former are more accurate than the latter.

Table 1

Natural frequencies for an isotropic F-F-F-F square plate (a/b=1, v=0.3).

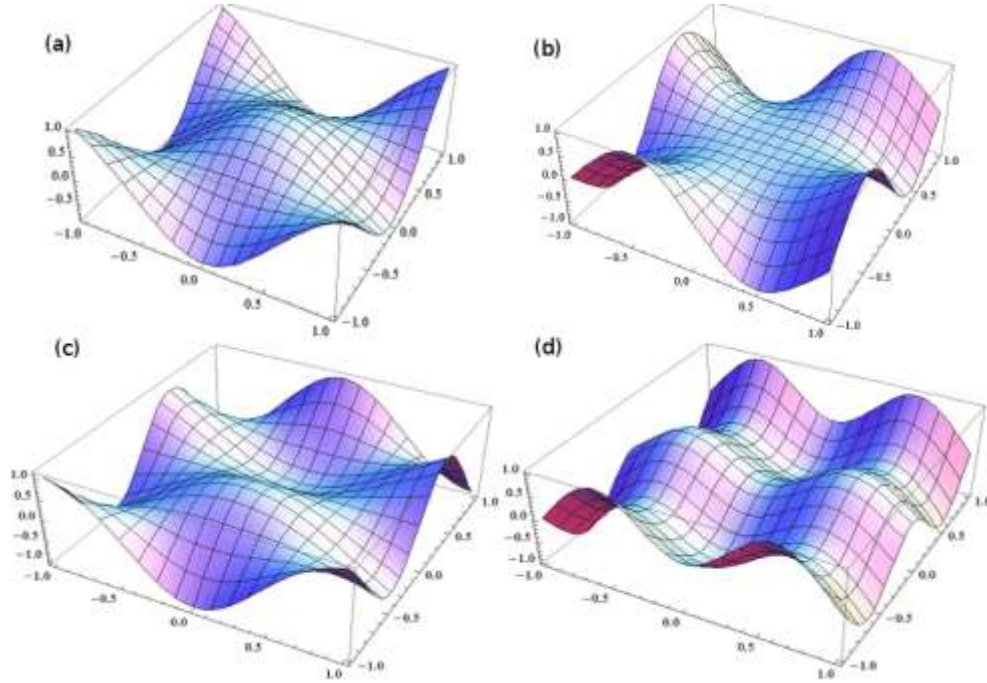| frequency No.	(k,j)	$\Omega = \sqrt[4]{\rho h \omega^2 / D}$		
		$N = 4$	$N = 10$	Papkov and Meleshko [36]
1	(1,1)	1.83499	1.83495	1.8350
2	(0,0)	2.21337	2.21337	2.2134
3	(0,0)	2.46326	2.46324	2.4633
4	(0,1)/(1,0)	2.94988	2.94961	2.9496
5	(0,1)/(1,0)	3.90811	3.90816	3.9081
6	(0,0)	3.99119	3.99020	3.9902
7	(1,1)	4.16138	4.16129	4.1613
8	(1,1)	4.39284	4.39239	4.3924
9	(0,1)/(1,0)	5.13540	5.13472	5.1347
10	(0,0)	5.42267	5.41083	5.4108

Fig. 4 Representative mode shapes with a/b=1 , v=0.3 for an isotropic plate with completely free boundary conditions (F-F-F-F). (a), (b), (c) and (d) are respectively for the sixth, seventh, ninth and tenth mode shapes.

Table 2

Natural frequency parameter λ for an isotropic F-F-F-F square plate ($a/b=1$, $v=0.3$).

frequency No.	(k,j)	$\lambda = 4\Omega^2 = 4\sqrt[4]{\dfrac{\rho h \omega^2}{D}}$	
		$N = 10$	Leissa [7]
1	(1,1)	13.4682	13.4728
2	(0,0)	19.5960	19.5961
3	(0,0)	24.2702	24.2702
4	(0,1)/(1,0)	34.8008	34.8011
5	(0,1)/(1,0)	61.0949	61.0932
6	(0,0)	63.6868	63.6870
7	(1,1)	69.2653	69.5020
8	(1,1)	77.1724	77.5897
9	(0,1)/(1,0)	105.461	105.463
10	(0,0)	117.108	117.109

Next, the natural frequencies of the F-F-F-F rectangular plate with $a/b=2$ have been computed using the proposed DSM and are compared with results based on the analytical method put forward by Papkov and Meleshko [36], see Table 3. The comparison suggests that the agreement is almost total. Again, a high rate of convergence can be observed in terms of number of terms N used in the series expansion. A comparison between Table 1 and Table 3 results reveals that the dimensionless natural frequencies of the rectangular plate ($a/b=2$) are lower than those of the square plate ($a/b=1$) which due to the nondimensionalisation used, is expected. Some representative mode shapes for this rectangular plate are illustrated in Fig. 5, which highlights different symmetric/anti-symmetric deformation behaviour similar to those of the square plate. The sixth mode shape (see Fig. 5(a)) is clearly doubly antisymmetric. On the other hand, the ninth mode is doubly symmetric (see Fig. 5(c)). By contrast, the seventh mode shape is symmetric (Fig. 5(b)) in y direction, but antisymmetric in x direction whereas the tenth one is symmetric in x but antisymmetric in y, see Fig. 5(d).

Table 3

Dimensionless natural frequencies for an isotropic F-F-F-F rectangular plate with $a/b=2$, $v=0.3$.

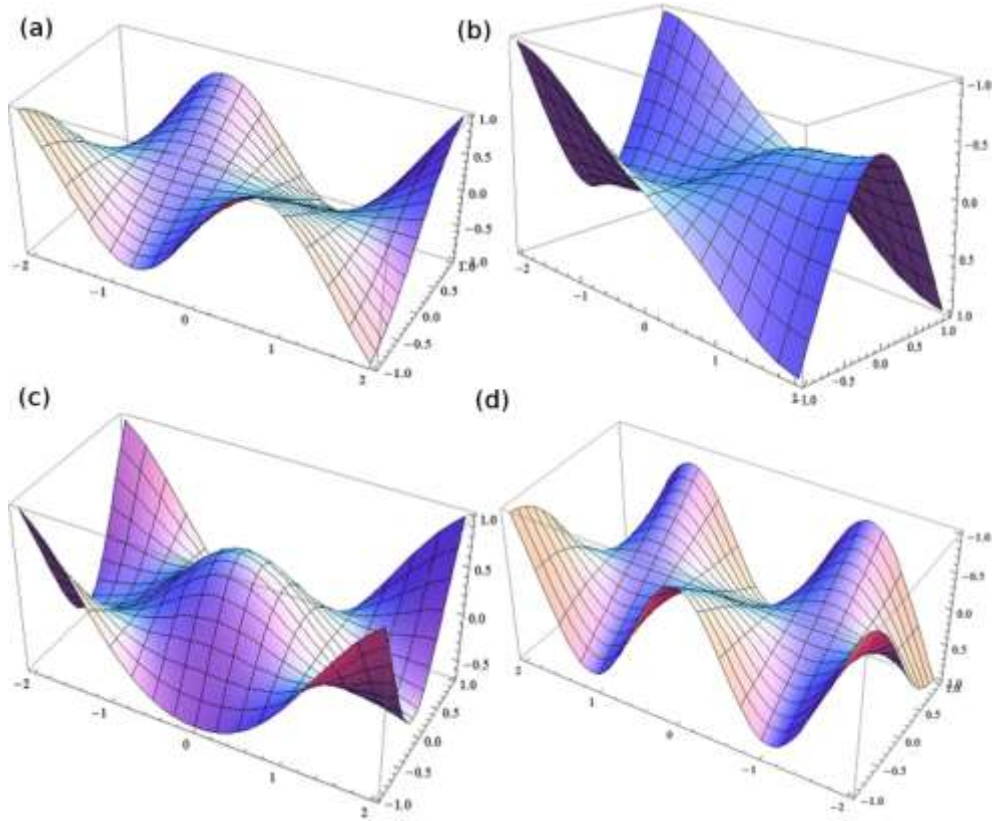| frequency No.	(k,j)	$\Omega = \sqrt[4]{\dfrac{\rho h \omega^2}{D}}$		
		$N = 4$	$N = 10$	Papkov and Meleshko [36]
1	(0,0)	1.15821	1.15821	1.1582
2	(1,1)	1.28880	1.28877	1.2888
3	(0,1)	1.91185	1.91132	1.9113
4	(1,0)	1.93014	1.93012	1.9301
5	(0,0)	2.34538	2.34534	2.3453
6	(1,1)	2.51932	2.51873	2.5187
7	(1,0)	2.54960	2.54954	2.5495
8	(0,0)	2.73240	2.72404	2.7240
9	(0,0)	3.00405	3.00190	3.0019
10	(0,1)	3.12925	3.16428	3.1642

Fig. 5 Representative mode shapes of an isotropic plate with a/b =2, v=0.3 for completely free boundary conditions (F-F-F-F). (a), (b), (c) and (d) are respectively for the sixth, seventh, ninth and tenth mode shapes.

Table 4

Non-dimensional natural frequencies for square and rectangular isotropic C-C-C-C plates with N =10.

frequency No.	$\Omega = \sqrt[4]{\dfrac{\rho h \omega^2}{D}}$	
	a/b=1	a/b=2
1	2.99937	2.47878
2	4.28351	2.82071
3	5.20117	3.34550
4	5.73543	3.97882
5	5.74901	3.99948
6	6.42227	4.21531
7	7.25449	4.56256
8	7.79612	4.67044
9	8.60721	5.01918
10	8.78778	5.39345

Table 5

Comparison of calculated frequency parameter λ for the doubly-symmetric modes of isotropic C-C-C-C square plate with $a/b=1$ with lower and upper bounds by Bazley, *et al* [42].

frequency	$\lambda = 4\Omega^2$		
No.	$N = 10$	lower Bounds	upper Bounds
1	35.9849	35.976	35.985
2	131.581	131.50	131.58
3	132.204	132.13	132.21
4	220.031	219.08	220.06
5	308.900	308.60	308.91
6	309.162	308.99	309.17
7	392.761	388.74	392.85
8	393.896	391.40	393.98
9	562.107	544.75	562.38
10	565.536	564.99	565.40

Table 6

Natural frequencies for square and rectangular plates ($v=0.3$) with C-F-C-F boundary conditions.

frequency	$\Omega = \sqrt[4]{\dfrac{\rho h \omega^2}{D}}$	
No.	$a/b=1$	$a/b=2$
1	2.35358	1.17339
2	2.56910	1.49878
3	3.30110	1.94881
4	3.91051	2.26837
5	4.09764	2.61525
6	4.46685	2.73200
7	4.67927	3.00721
8	5.47793	3.15171
9	5.57778	3.75078
10	5.62793	3.77386

Table 7

Comparison of natural frequency parameter λ for the doubly symmetric modes of a square and rectangular plate ($v=0.3$) with C-F-C-F boundary conditions with those of Claassen and Thorne [43].

frequency No.		$\lambda = 4\Omega^2$	
		$N = 10$	Claassen & Thorne [42]
$a/b=1$	1	22.165	22.17
	2	43.589	43.6
	3	120.09	120.1
	4	136.89	136.9
	5	149.29	149.3
$a/b=2$	1	5.5074	5.51
	2	27.358	27.3
	3	29.855	29.9
	4	56.968	56.9
	5	73.968	74.0

To demonstrate the method, further results with other boundary conditions were computed. Table 4 shows the first ten natural frequencies $\Omega = \sqrt[4]{\rho h \omega^2 / D}$ of both the square plate (*a/b*=1) and the rectangular plate (*a/b*=2) but with all round clamped edges (C-C-C-C). The number of terms *N* included in the series expansion was fixed at 10. For similar reason as explained for the F-F-F-F case, it is expected that the dimensionless natural frequencies of a rectangular plate are lower than those of a square one. In Table 5, the results for the frequency parameter $\lambda = 4\Omega^2$ are validated by the lower and upper bounds of this particular problem given by Bazeley *et.al.* [42]. Results from the present theory are between the lower and upper bounds of Ref. [42] in almost all cases.

Following the validation of results (see Table 3, and 5), Table 6 shows the next set of results for a square (*a/b*=1) and a rectangular plate (*a/b*=2) with C-F-C-F boundary conditions. Similar results for this set of boundary conditions are shown in Table 7 alongside the results of Claassen and Thorne [43] for a direct comparison.

The results for both square and rectangular plates with completely free edges clearly demonstrate rapid convergence with respect to the number of terms used in the series, see Table 1 and 3. This is in accord with the assertion made by Kantorovich and Krylov [39] who concluded that Fourier series will be rapidly convergent if the function itself and a certain number of its first derivatives are continuous and periodic. This is surely the case for the free vibration analysis of plates for most of the practical cases where the deflection and its first three derivatives are generally continuous functions and essentially periodic. (For a plate with combined and piecewise displacement and force boundary conditions, the approximation in the discontinuities can be avoided by partitioning the plate into two-dimensional assembly of plate elements, which will facilitate the application of the boundary conditions considerably.)

The comparison of results with published results shows the high accuracy and computational efficiency of the proposed method. Excellent agreement for the free vibration of thin plates with completely free edges (F-F-F-F) was achieved when compared with regularity analysis of infinite system by Papkov [36], and the Rayleigh-Ritz method by Lessia [7]. The mode shape computation of a square plate with F-F-F-F boundary conditions using the present method gives results that are in accord with the well-known Chaldni figures [1] exhibiting both symmetric and anti-symmetric properties of the plate's dynamic behaviour. For C-C-C-C and C-F-C-F boundary conditions, the results computed using the proposed method are in excellent agreement with published results [42, 43].

Any possible numerical inaccuracy in the current study has been effectively eliminated significantly in that the unknown coefficients are eliminated from the boundary conditions for rotations and shear forces, rather than eliminating them by the matrix inversion, i.e., using the formulation $\mathbf{K} = \mathbf{R}\mathbf{A}^{-1}$ which is commonly used by researchers in the dynamic stiffness formulation [33]. (The inverse of the matrix $\mathbf{A}$ may cause numerical ill-

conditioning and thus can introduce errors in the results of computation [44].) The high accuracy of the current method also stems from the improved reduced system of infinite system by using the generalised limitant theory proposed by Papkov [37]. The truncation of the infinite system due to the introduction of general solution in series form can introduce error in the computed results. This type of error has been diminished, if not practically eliminated in the present method by the use of the limitant theory [37] when developing the DS matrix.

4. Conclusions

An exact dynamic stiffness (DS) matrix has been developed for a rectangular plate for the most general case. This has been achieved by obtaining an infinite series general solution which satisfies the governing differential equations exactly. Following lengthy symbolic manipulations (both by hand and by symbolic computation), the frequency dependent DS matrix has been obtained by eliminating the unknown coefficients in the general solution when the plate is free on all its edges. Even though series solution has been used in the formulation, to all intents and purposes, the DS matrix is nevertheless, exact or almost exact because of the use of the generalised limitant theory [37] which eliminates the truncation errors. The formulated DS matrix represents the force-displacement relationship of a thin plate for the general case when the plate is undergoing free vibration. The prescribed boundary conditions for displacements and forces are represented by Fourier series to give any arbitrarily chosen accuracy. The well-established Wittrick-Williams (WW) algorithm was applied as solution technique to compute the natural frequencies. The corresponding mode shapes are recovered from the usual eigensolution procedure. The cumbersome j_0 count of the WW algorithm is resolved by taking advantage of the nature of the series-form solution to ensure that the j_0 count is always zero for a given trial frequency. The natural frequencies and representative mode shapes for both square and rectangular plates for a wide range of boundary conditions have been computed and a substantial amount of results are validated against published results. The high accuracy and elegance of the proposed method have been demonstrated.

This investigation has removed the previous restriction of the dynamic stiffness method applications which was confined to plates with at least two opposite sides simply supported. The development of general purpose computer programs using the DSM is now possible as a result of the current investigation. Such programs will be vastly more accurate and computationally efficient in computer-aided structural analysis and design when compared with the traditional finite element method. It is envisaged that the research reported in this paper will spark a paradigm change in solving complex elastodynamic problems in an accurate and computationally efficient manner.

Appendix A. Infinite system of algebraic equations for the doubly symmetric component case ($k=j=0$).

This appendix shows the procedure for generating the infinite system of linear algebraic equation for the doubly symmetric component case, i.e., $k=j=0$ of Eq. (10). By substituting Eqs. (34)-(35) into Eqs. (11), (24) and (25), the following equalities are obtained after some algebraic manipulation using symbolic computation.

$$
\begin{aligned}
W^{00}(a,y) &= W_{1_0} + \sum_{n=1}^{\infty} W_{1_n} \cos\beta_n y = \\
&\frac{\phi_{y_0}(\cot\Omega a - \coth\Omega a)}{2\Omega} + \frac{V_{x_0}(\cot\Omega a + \coth\Omega a)}{2\Omega^3} + \frac{\phi_{x_0}}{2\Omega}\left(\frac{\cos\Omega y}{\sin\Omega b} - \frac{\cosh\Omega y}{\sinh\Omega b}\right) + \frac{V_{y_0}}{2\Omega^3}\left(\frac{\cos\Omega y}{\sin\Omega b} + \frac{\cosh\Omega y}{\sinh\Omega b}\right) \\
&+ \sum_{n=1}^{\infty}\left(\phi_{y_n}\left\{\frac{q_{1n}^2 - (2-\nu)\beta_n^2}{q_{2n}}\coth q_{2n}a - \frac{q_{2n}^2 - (2-\nu)\beta_n^2}{q_{1n}}\coth q_{1n}a\right\} + V_{x_n}\left\{\frac{\coth q_{2n}a}{q_{2n}} - \frac{\coth q_{1n}a}{q_{1n}}\right\}\right)\frac{\cos\beta_n y}{2\Omega^2} \\
&+ \sum_{n=1}^{\infty}\frac{(-1)^n}{2\Omega^2}\left(-\phi_{x_n}\left\{\frac{p_{2n}^2-(2-\nu)\alpha_n^2}{p_{1n}}\frac{\cosh p_{1n}y}{\sinh p_{1n}b} - \frac{p_{1n}^2-(2-\nu)\alpha_n^2}{p_{2n}}\frac{\cosh p_{2n}y}{\sinh p_{2n}b}\right\} + V_{y_n}\left\{\frac{\cosh p_{2n}y}{p_{2n}\sinh p_{2n}b} - \frac{\cosh p_{1n}y}{p_{1n}\sinh p_{1n}b}\right\}\right)
\end{aligned}
$$

(A.1)

$$
\begin{aligned}
W^{00}(x,a) &= W_{2_0} + \sum_{n=1}^{\infty} W_{2_n}\cos\alpha_n x = \\
&\frac{\phi_{y_0}}{2\Omega}\left(\frac{\cos\Omega x}{\sin\Omega a} - \frac{\cosh\Omega x}{\sinh\Omega a}\right) + \frac{V_{x_0}}{2\Omega^3}\left(\frac{\cos\Omega x}{\sin\Omega a} + \frac{\cosh\Omega x}{\sinh\Omega a}\right) + \frac{\phi_{x_0}(\cot\Omega b - \coth\Omega b)}{2\Omega} + \frac{V_{y_0}(\cot\Omega b + \coth\Omega b)}{2\Omega^3} \\
&+ \sum_{n=1}^{\infty}\frac{(-1)^{n+1}}{2\Omega^2}\left(\phi_{y_n}\left\{\frac{q_{2n}^2-(2-\nu)\beta_n^2}{q_{1n}}\frac{\cosh q_{1n}x}{\sinh q_{1n}a} - \frac{q_{1n}^2-(2-\nu)\beta_n^2}{q_{2n}}\frac{\cosh q_{2n}x}{\sinh q_{2n}a}\right\} - V_{x_n}\left\{\frac{\cosh q_{2n}x}{q_{2n}\sinh q_{2n}a} - \frac{\cosh q_{1n}x}{q_{1n}\sinh q_{1n}a}\right\}\right) \\
&+ \sum_{n=1}^{\infty}\left(\phi_{x_n}\left\{\frac{p_{1n}^2-(2-\nu)\alpha_n^2}{p_{2n}}\coth p_{2n}b - \frac{p_{2n}^2-(2-\nu)\alpha_n^2}{p_{1n}}\coth p_{1n}b\right\} + V_{y_n}\left\{\frac{\coth p_{2n}b}{p_{2n}} - \frac{\coth p_{1n}b}{p_{1n}}\right\}\right)\frac{\cos\alpha_n x}{2\Omega^2}
\end{aligned}
$$

(A.2)

$$
\begin{aligned}
-M_x^{00}(a,y)/D &= M_{x_0} + \sum_{n=1}^{\infty} M_{x_n}\cos\beta_n y = \\
&-\frac{\Omega\phi_{y_0}(\cot\Omega a + \coth\Omega a)}{2} - \frac{V_{x_0}(\cot\Omega a - \coth\Omega a)}{2\Omega} - \frac{\nu\Omega\phi_{x_0}}{2}\left(\frac{\cos\Omega y}{\sin\Omega b} + \frac{\cosh\Omega y}{\sinh\Omega b}\right) - \frac{\nu V_{y_0}}{2\Omega}\left(\frac{\cos\Omega y}{\sin\Omega b} - \frac{\cosh\Omega y}{\sinh\Omega b}\right) \\
&+ \sum_{n=1}^{\infty}\left(\phi_{y_n}\left\{\frac{(q_{1n}^2-(2-\nu)\beta_n^2)(q_{2n}^2-\nu\beta_n^2)}{q_{2n}}\coth q_{2n}a - \frac{(q_{2n}^2-(2-\nu)\beta_n^2)(q_{1n}^2-\nu\beta_n^2)}{q_{1n}}\coth q_{1n}a\right\}\right. \\
&\left.+ V_{x_n}\left\{\frac{q_{2n}^2-\nu\beta_n^2}{q_{2n}}\coth q_{2n}a - \frac{q_{1n}^2-\nu\beta_n^2}{q_{1n}}\coth q_{1n}a\right\}\right)\frac{\cos\beta_n y}{2\Omega^2} + \sum_{n=1}^{\infty}\frac{(-1)^n}{2\Omega^2}\left(\phi_{x_n}\left\{\frac{(p_{1n}^2-(2-\nu)\alpha_n^2)(\nu p_{2n}^2-\alpha_n^2)}{p_{2n}}\right.\right. \\
&\left.\times\frac{\cosh p_{2n}y}{\sinh p_{2n}b} - \frac{(p_{2n}^2-(2-\nu)\alpha_n^2)(\nu p_{1n}^2-\alpha_n^2)}{p_{1n}}\frac{\cosh p_{1n}y}{\sinh p_{1n}b}\right\} + V_{y_n}\left\{\frac{\nu p_{2n}^2-\alpha_n^2}{p_{2n}}\frac{\cosh p_{2n}y}{\sinh p_{2n}b} - \frac{\nu p_{1n}^2-\alpha_n^2}{p_{1n}}\frac{\cosh p_{1n}y}{\sinh p_{1n}b}\right\}\right)
\end{aligned}
$$

(A.3)

$$-M_y^{00}(x,b)/D = -M_{y_0} - \sum_{n=1}^{\infty} M_{y_n}\cos\alpha_n x =$$

$$-\frac{\nu\,\Omega\phi_{y_0}}{2}\left(\frac{\cos\Omega x}{\sin\Omega a} + \frac{\cosh\Omega x}{\sinh\Omega a}\right) - \frac{\nu\,V_{x_0}}{2\Omega}\left(\frac{\cos\Omega x}{\sin\Omega a} - \frac{\cosh\Omega x}{\sinh\Omega a}\right) - \frac{\Omega\phi_{x_0}(\cot\Omega b + \coth\Omega b)}{2} - \frac{V_{y_0}(\cot\Omega b - \coth\Omega b)}{2\Omega}$$

$$+\sum_{n=1}^{\infty}\frac{(-1)^n}{2\Omega^2}\left(\phi_{y_n}\left\{\frac{(q_{1n}^2-(2-\nu)\beta_n^2)(\nu q_{2n}^2-\beta_n^2)}{q_{2n}}\frac{\cosh q_{2n}x}{\sinh q_{2n}a} - \frac{(q_{2n}^2-(2-\nu)\beta_n^2)(\nu q_{1n}^2-\beta_n^2)}{q_{1n}}\frac{\cosh q_{1n}x}{\sinh q_{1n}a}\right\}\right.$$

$$\left.+V_{x_n}\left\{\frac{\nu q_{2n}^2-\beta_n^2}{q_{2n}}\frac{\cosh q_{2n}x}{\sinh q_{2n}a} - \frac{\nu q_{1n}^2-\beta_n^2}{q_{1n}}\frac{\cosh q_{1n}x}{\sinh q_{1n}a}\right\}\right) + \sum_{n=1}^{\infty}\left(\phi_{x_n}\left\{\frac{(p_{1n}^2-(2-\nu)\alpha_n^2)(p_{2n}^2-\nu\alpha_n^2)}{p_{2n}}\coth p_{2n}b\right.\right.$$

$$\left.\left.-\frac{(p_{2n}^2-(2-\nu)\alpha_n^2)(p_{1n}^2-\nu\alpha_n^2)}{p_{1n}}\coth p_{1n}b\right\}+V_{y_n}\left\{\left\{\frac{p_{2n}^2-\nu\alpha_n^2}{p_{2n}}\coth p_{2n}b - \frac{p_{1n}^2-\nu\alpha_n^2}{p_{1n}}\coth p_{1n}b\right\}\right)\right)\frac{\cos\alpha_n x}{2\Omega^2}$$

$$\text{(A.4)}$$

Expanding the ratios of the hyperbolic functions in Eqs. (A.1)-(A.4) into Fourier series form (see Appendix **B**) and changing the order of summation lead to an infinite system of linear algebraic equations relating Fourier coefficients of the boundary displacements $W_{1n}, \phi_{y_n}, W_{2n}, \phi_{x_n}$ and the boundary forces $V_{x_n}, M_{x_n}, V_{y_n}, M_{y_n}$ as follows:

$$\frac{\cot\Omega a + \coth\Omega a}{2\Omega^3}V_{x_0} + \frac{1}{b\Omega^4}V_{y_0} - W_{1_0} + \frac{\cot\Omega a - \coth\Omega a}{2\Omega}\phi_{y_0} = \sum_{n=1}^{\infty}\frac{(-1)^n}{bp_{1n}^2p_{2n}^2}\left(V_{y_n}+\nu\alpha_n^2\phi_{x_n}\right)$$

$$\text{(A.5)}$$

$$\frac{1}{a\Omega^4}V_{x_0} + \frac{\cot\Omega b + \coth\Omega b}{2\Omega^3}V_{y_0} - W_{2_0} + \frac{\cot\Omega b - \coth\Omega b}{2\Omega}\phi_{x_0} = \sum_{n=1}^{\infty}\frac{(-1)^n}{aq_{1n}^2q_{2n}^2}\left(V_{x_n}+\nu\beta_n^2\phi_{y_n}\right)$$

$$\text{(A.6)}$$

$$M_{x_0} + \frac{\cot\Omega a - \coth\Omega a}{2\Omega}V_{x_0} + \frac{\Omega(\cot\Omega a + \coth\Omega a)}{2}\phi_{y_0} + \frac{\nu}{b}\phi_{x_0} = \sum_{n=1}^{\infty}\frac{(-1)^n}{bp_{1n}^2p_{2n}^2}\left(\alpha_n^2V_{y_n}+\nu\Omega^4\phi_{x_n}\right)$$

$$\text{(A.7)}$$

$$M_{y_0} + \frac{\cot\Omega b - \coth\Omega b}{2\Omega}V_{y_0} + \frac{\nu}{a}\phi_{y_0} + \frac{\Omega(\cot\Omega b + \coth\Omega b)}{2}\phi_{x_0} = \sum_{n=1}^{\infty}\frac{(-1)^n}{aq_{1n}^2q_{2n}^2}\left(\beta_n^2V_{x_n}+\nu\Omega^4\phi_{y_n}\right)$$

$$\text{(A.8)}$$

$$\Delta_{2m}V_{x_m} - 2\Omega^2W_{1_m} + \Delta_{1m}\phi_{y_m} = \frac{4\Omega^2(-1)^m}{bq_{1m}^2q_{2m}^2}\left(V_{y_0}+\beta_m^2\phi_{x_0}\right) + \frac{4\Omega^2}{b}\sum_{n=1}^{\infty}\frac{(-1)^{m+n}\left(V_{y_n}+(\beta_m^2+\nu\alpha_n^2)\phi_{x_n}\right)}{(\alpha_n^2+q_{1m}^2)(\alpha_n^2+q_{2m}^2)}$$

$$\text{(A.9)}$$

$$\Delta_{4m}V_{y_m} - 2\Omega^2W_{2_m} + \Delta_{3m}\phi_{x_m} = \frac{4\Omega^2(-1)^m}{ap_{1m}^2p_{2m}^2}\left(V_{x_0}+\alpha_m^2\phi_{y_0}\right) + \frac{4\Omega^2}{a}\sum_{n=1}^{\infty}\frac{(-1)^{m+n}\left(V_{x_n}+(\alpha_m^2+\nu\beta_n^2)\phi_{y_n}\right)}{(\beta_n^2+p_{1m}^2)(\beta_n^2+p_{2m}^2)}$$

$$\text{(A.10)}$$

$$2\Omega^2M_{x_m} - \Delta_{6m}V_{x_m} + \Delta_{5m}\phi_{y_m} = \frac{4\nu\Omega^2(-1)^m}{bq_{1m}^2q_{2m}^2}\left(\beta_m^2V_{y_0}+\Omega^4\phi_{x_0}\right)$$

$$+\frac{4\Omega^2}{b}\sum_{n=1}^{\infty}\frac{(-1)^{m+n}\left(\left(\nu\beta_m^2+\alpha_n^2\right)V_{y_n}+\left((1-\nu)^2\beta_m^2\alpha_n^2+\nu\Omega^4\right)\phi_{x_n}\right)}{(\alpha_n^2+q_{1m}^2)(\alpha_n^2+q_{2m}^2)}$$

$$\text{(A.11)}$$

29

$$2\Omega^2 M_{y_m} - \Delta_{8m} V_{y_m} + \Delta_{7m}\phi_{x_m} = \frac{4\nu\Omega^2(-1)^m}{ap_{1m}^2 p_{2m}^2}\left(\alpha_m^2 V_{x_0} + \Omega^4 \phi_{y_0}\right)$$

$$+ \frac{4\Omega^2}{a}\sum_{n=1}^{\infty} \frac{(-1)^{m+n}\left(\left(\nu\alpha_m^2 + \beta_n^2\right)V_{x_n} + \left((1-\nu)^2\alpha_m^2\beta_n^2 + \nu\Omega^4\right)\phi_{y_n}\right)}{(\beta_n^2 + p_{1m}^2)(\beta_n^2 + p_{2m}^2)} \tag{A.12}$$

where the expressions for Δ_{jm} ($j = 1, 2, 3\ldots8$) are given below.

$$\Delta_{1n} = \frac{q_{1n}^2 - (2-\nu)\beta_n^2}{q_{2n}}\coth q_{2n}a - \frac{q_{2n}^2 - (2-\nu)\beta_n^2}{q_{1n}}\coth q_{1n}a \tag{A.13}$$

$$\Delta_{2n} = \frac{\coth q_{2n}a}{q_{2n}} - \frac{\coth q_{1n}a}{q_{1n}} \tag{A.14}$$

$$\Delta_{3n} = \frac{p_{1n}^2 - (2-\nu)\alpha_n^2}{p_{2n}}\coth p_{2n}b - \frac{p_{2n}^2 - (2-\nu)\alpha_n^2}{p_{1n}}\coth p_{1n}b \tag{A.15}$$

$$\Delta_{4n} = \frac{\coth p_{2n}b}{p_{2n}} - \frac{\coth p_{1n}b}{p_{1n}} \tag{A.16}$$

$$\Delta_{5n} = \frac{(q_{2n}^2 - (2-\nu)\beta_n^2)(q_{1n}^2 - \nu\beta_n^2)}{q_{1n}}\coth q_{1n}a - \frac{(q_{1n}^2 - (2-\nu)\beta_n^2)(q_{2n}^2 - \nu\beta_n^2)}{q_{2n}}\coth q_{2n}a \tag{A.17}$$

$$\Delta_{6n} = \frac{q_{2n}^2 - \nu\beta_n^2}{q_{2n}}\coth q_{2n}a - \frac{q_{1n}^2 - \nu\beta_n^2}{q_{1n}}\coth q_{1n}a \tag{A.18}$$

$$\Delta_{7n} = \frac{(p_{2n}^2 - (2-\nu)\alpha_n^2)(p_{1n}^2 - \nu\alpha_n^2)}{p_{1n}}\coth p_{1n}b - \frac{(p_{1n}^2 - (2-\nu)\alpha_n^2)(p_{2n}^2 - \nu\alpha_n^2)}{p_{2n}}\coth p_{2n}b \tag{A.19}$$

$$\Delta_{8n} = \frac{p_{2n}^2 - \nu\alpha_n^2}{p_{2n}}\coth p_{2n}b - \frac{p_{1n}^2 - \nu\alpha_n^2}{p_{1n}}\coth p_{1n}b \tag{A.20}$$

Note that this appendix only for the doubly-symmetric component case. The equivalent expressions for the remaining three cases are recorded in Appendix **C**.

Appendix B. Fourier series relationships of hyperbolic and trigonometric functions.

Some well-known expansions of ratios of hyperbolic and trigonometric functions for expanding Eqs. (A.1)-(A.4) into Fourier series are given below in order to make the paper self-contained.

$$\frac{\cosh py}{\sinh pb} = \frac{1}{pb} + \frac{2p}{b} \sum_{m=1}^{\infty} \frac{(-1)^m \cos \beta_m y}{\beta_m^2 + p^2} \tag{B.1}$$

$$\frac{\cos \Omega y}{\sin \Omega b} - \frac{\cosh \Omega y}{\sinh \Omega b} = \frac{4\Omega}{b} \sum_{m=1}^{\infty} \frac{(-1)^{m+1} \beta_m^2 \cos \beta_m y}{q_{1m}^2 q_{2m}^2} \tag{B.2}$$

$$\frac{\cos \Omega y}{\sin \Omega b} + \frac{\cosh \Omega y}{\sinh \Omega b} = \frac{2}{\Omega b} + \frac{4\Omega^3}{b} \sum_{m=1}^{\infty} \frac{(-1)^{m+1} \cos \beta_m y}{q_{1m}^2 q_{2m}^2} \tag{B.3}$$

$$\frac{p_{2n}^2 - (2-v)\alpha_n^2}{p_{1n}} \frac{\cosh p_{1n} y}{\sinh p_{1n} b} - \frac{p_{1n}^2 - (2-v)\alpha_n^2}{p_{2n}} \frac{\cosh p_{2n} y}{\sinh p_{2n} b} = \frac{2v\Omega^2 \alpha_n^2}{bp_{1n}^2 p_{2n}^2} + \frac{4\Omega^2}{b} \sum_{m=1}^{\infty} \frac{(-1)^m (\beta_m^2 + v\alpha_n^2) \cos \beta_m y}{(\beta_m^2 + p_{1n}^2)(\beta_m^2 + p_{2n}^2)} \tag{B.4}$$

$$\frac{\cosh p_{2n} y}{p_{2n} \sinh p_{2n} b} - \frac{\cosh p_{1n} y}{p_{1n} \sinh p_{1n} b} = -\frac{2\Omega^2}{bp_{1n}^2 p_{2n}^2} - \frac{4\Omega^2}{b} \sum_{m=1}^{\infty} \frac{(-1)^m \cos \beta_m y}{(\beta_m^2 + p_{1n}^2)(\beta_m^2 + p_{2n}^2)} \tag{B.5}$$

$$\frac{(p_{1n}^2 - (2-v)\alpha_n^2)(v p_{2n}^2 - \alpha_n^2)}{p_{2n}} \frac{\cosh p_{2n} y}{\sinh p_{2n} b} - \frac{(p_{2n}^2 - (2-v)\alpha_n^2)(v p_{1n}^2 - \alpha_n^2)}{p_{1n}} \frac{\cosh p_{1n} y}{\sinh p_{1n} b} = \frac{2v\Omega^6}{bp_{1n}^2 p_{2n}^2}$$
$$+ \frac{4\Omega^2}{b} \sum_{m=1}^{\infty} \frac{(-1)^m \left\{ (1-v)^2 \alpha_n^2 \beta_m^2 + v\Omega^4 \right\} \cos \beta_m y}{(\beta_m^2 + p_{1n}^2)(\beta_m^2 + p_{2n}^2)} \tag{B.6}$$

$$\frac{v p_{2n}^2 - \alpha_n^2}{p_{2n}} \frac{\cosh p_{2n} y}{\sinh p_{2n} b} - \frac{v p_{1n}^2 - \alpha_n^2}{p_{1n}} \frac{\cosh p_{1n} y}{\sinh p_{1n} b} = \frac{2\Omega^2 \alpha_n^2}{bp_{1n}^2 p_{2n}^2} + \frac{4\Omega^2}{b} \sum_{m=1}^{\infty} \frac{(-1)^m (v\beta_m^2 + \alpha_n^2) \cos \beta_m y}{(\beta_m^2 + p_{1n}^2)(\beta_m^2 + p_{2n}^2)} \tag{B.7}$$

Parallel expressions can be obtained for the hyperbolic functions in the Eqs. (B.1)-(B.7) by interchanging the symbols and following the scheme shown below

$$y \leftrightarrow x, \quad b \leftrightarrow a, \quad \beta_m \leftrightarrow \alpha_m, \quad \alpha_n \leftrightarrow \beta_n, \quad p_{jn} \leftrightarrow q_{jn}, \quad q_{jm} \leftrightarrow p_{jm}. \tag{B.8}$$

Appendix C. Infinite system of algebraic equations for the remaining symmetric and anti-symmetric component cases.

The boundary sub-vectors of displacements and forces for other component cases of symmetry are connected by similar relationships like Eqs. (19)- (29). In particular, for even function in direction Ox and odd function in direction Oy, these sub-vectors can be expanded as

$$\mathbf{d}^{01} = \begin{bmatrix} \sum_{n=1}^{\infty} W_{1_n} \sin \tilde{\beta}_n y \\ \sum_{n=1}^{\infty} \phi_{y_n} \sin \tilde{\beta}_n y \\ W_{2_0} + \sum_{n=1}^{\infty} W_{2_n} \cos \alpha_n x \\ -\phi_{x_0} - \sum_{n=1}^{\infty} \phi_{x_n} \cos \alpha_n x \end{bmatrix} ; \quad \mathbf{f}^{01} = -D \begin{bmatrix} \sum_{n=1}^{\infty} V_{x_n} \sin \tilde{\beta}_n y \\ \sum_{n=1}^{\infty} M_{x_n} \sin \tilde{\beta}_n y \\ V_{y_0} + \sum_{n=1}^{\infty} V_{y_n} \cos \alpha_n x \\ -M_{y_0} - \sum_{n=1}^{\infty} M_{y_n} \cos \alpha_n x \end{bmatrix} \quad (C.1)$$

where Fourier coefficients are connected by follow equations as

$$\frac{\tan \Omega b - \tanh \Omega b}{2\Omega^3} V_{y0} + W_{20} + \frac{\tan \Omega b + \tanh \Omega b}{2\Omega} \phi_{x0} = \sum_{n=1}^{\infty} \frac{(-1)^n}{a \tilde{q}_{1n}^2 \tilde{q}_{2n}^2} \left(V_{x_n} + \nu \tilde{\beta}_n^2 \phi_{y_n} \right) \quad (C.2)$$

$$M_{y0} - \frac{\tan \Omega b + \tanh \Omega b}{2\Omega} V_{y0} - \frac{\Omega (\tan \Omega b - \tanh \Omega b)}{2} \phi_{x0} = \sum_{n=1}^{\infty} \frac{(-1)^{n+1}}{a \tilde{q}_{1n}^2 \tilde{q}_{2n}^2} \left(\tilde{\beta}_n^2 V_{x_n} + \nu \Omega^4 \phi_{y_n} \right) \quad (C.3)$$

$$\Delta_{2m}^{01} V_{x_m} - 2\Omega^2 W_{1_m} + \Delta_{1m}^{01} \phi_{y_m} = -\frac{4\Omega^2 (-1)^m}{b \tilde{q}_{1m}^2 \tilde{q}_{2m}^2} \left(V_{y0} + \tilde{\beta}_m^2 \phi_{x0} \right) - \frac{4\Omega^2}{b} \sum_{n=1}^{\infty} \frac{(-1)^{m+n} \left(V_{y_n} + (\tilde{\beta}_m^2 + \nu \alpha_n^2) \phi_{x_n} \right)}{(\alpha_n^2 + \tilde{q}_{1m}^2)(\alpha_n^2 + \tilde{q}_{2m}^2)} \quad (C.4)$$

$$\Delta_{4m}^{01} V_{y_m} - 2\Omega^2 W_{2_m} + \Delta_{3m}^{01} \phi_{x_m} = -\frac{4\Omega^2}{a} \sum_{n=1}^{\infty} \frac{(-1)^{m+n} \left(V_{x_n} + (\alpha_m^2 + \nu \tilde{\beta}_n^2) \phi_{y_n} \right)}{(\tilde{\beta}_n^2 + p_{1m}^2)(\tilde{\beta}_n^2 + p_{2m}^2)} \quad (C.5)$$

$$2\Omega^2 M_{x_m} - \Delta_{6m}^{01} V_{x_m} + \Delta_{5m}^{01} \phi_{y_m} = -\frac{4\nu \Omega^2 (-1)^m}{b \tilde{q}_{1m}^2 \tilde{q}_{2m}^2} \left(\tilde{\beta}_m^2 V_{y0} + \Omega^4 \phi_{x0} \right)$$
$$- \frac{4\Omega^2}{b} \sum_{n=1}^{\infty} \frac{(-1)^{m+n} \left((\nu \tilde{\beta}_m^2 + \alpha_n^2) V_{y_n} + ((1-\nu)^2 \tilde{\beta}_m^2 \alpha_n^2 + \nu \Omega^4) \phi_{x_n} \right)}{(\alpha_n^2 + \tilde{q}_{1m}^2)(\alpha_n^2 + \tilde{q}_{2m}^2)} \quad (C.6)$$

$$2\Omega^2 M_{y_m} - \Delta_{8m}^{01} V_{y_m} + \Delta_{7m}^{01} \phi_{x_m} = -\frac{4\Omega^2}{a} \sum_{n=1}^{\infty} \frac{(-1)^{m+n} \left((\nu \alpha_m^2 + \tilde{\beta}_n^2) V_{x_n} + ((1-\nu)^2 \alpha_m^2 \tilde{\beta}_n^2 + \nu \Omega^4) \phi_{y_n} \right)}{(\tilde{\beta}_n^2 + p_{1m}^2)(\tilde{\beta}_n^2 + p_{2m}^2)} \quad (C.7)$$

Here sequences Δ_{jm}^{01} (j=1, 2, ..., 8) can be obtained from Δ_{jm} (see appendix **B**) by interchanging the symbols following the scheme

$$\beta_m \to \tilde{\beta}_m; \ q_{jm} \to \tilde{q}_{jm}; \ \coth p_{jm}b \to \tanh p_{jm}b \tag{C.8}$$

In the odd function cases for both coordinates boundary displacements and forces can be expanded as

$$\mathbf{d}^{11} = \begin{bmatrix} \sum_{n=1}^{\infty} W_{1_n} \sin \tilde{\beta}_n y \\ \sum_{n=1}^{\infty} \phi_{y_n} \sin \tilde{\beta}_n y \\ \sum_{n=1}^{\infty} W_{2_n} \sin \tilde{\alpha}_n x \\ -\sum_{n=1}^{\infty} \phi_{x_n} \sin \tilde{\alpha}_n x \end{bmatrix}; \ \mathbf{f}^{11} = -D \cdot \begin{bmatrix} \sum_{n=1}^{\infty} V_{x_n} \sin \tilde{\beta}_n y \\ \sum_{n=1}^{\infty} M_{x_n} \sin \tilde{\beta}_n y \\ \sum_{n=1}^{\infty} V_{y_n} \sin \tilde{\alpha}_n x \\ -\sum_{n=1}^{\infty} M_{y_n} \sin \tilde{\alpha}_n x \end{bmatrix} \tag{C.9}$$

The infinite system relating the Fourier coefficients in such cases can be written as

$$\Delta_{2m}^{11} V_{x_m} - 2\Omega^2 W_{1m} + \Delta_{1m}^{11} \phi_{y_m} = \frac{4\Omega^2}{b} \sum_{n=1}^{\infty} \frac{(-1)^{m+n} \left(V_{y_n} + (\tilde{\beta}_m^2 + \nu \tilde{\alpha}_n^2) \phi_{x_n} \right)}{(\tilde{\alpha}_n^2 + \tilde{q}_{1m}^2)(\tilde{\alpha}_n^2 + \tilde{q}_{2m}^2)} \tag{C.10}$$

$$\Delta_{4m}^{11} V_{y_m} - 2\Omega^2 W_{2m} + \Delta_{3m}^{11} \phi_{x_m} = \frac{4\Omega^2}{a} \sum_{n=1}^{\infty} \frac{(-1)^{m+n} \left(V_{x_n} + (\tilde{\alpha}_m^2 + \nu \tilde{\beta}_n^2) \phi_{y_n} \right)}{(\tilde{\beta}_n^2 + \tilde{p}_{1m}^2)(\tilde{\beta}_n^2 + \tilde{p}_{2m}^2)} \tag{C.11}$$

$$2\Omega^2 M_{x_m} - \Delta_{6m}^{11} V_{x_m} + \Delta_{5m}^{11} \phi_{y_m} = \frac{4\Omega^2}{b} \sum_{n=1}^{\infty} \frac{(-1)^{m+n} \left(\left(\nu \tilde{\beta}_m^2 + \tilde{\alpha}_n^2\right) V_{y_n} + \left((1-\nu)^2 \tilde{\beta}_m^2 \tilde{\alpha}_n^2 + \nu \Omega^4\right) \phi_{x_n} \right)}{(\tilde{\alpha}_n^2 + \tilde{q}_{1m}^2)(\tilde{\alpha}_n^2 + \tilde{q}_{2m}^2)} \tag{C.12}$$

$$2\Omega^2 M_{y_m} - \Delta_{8m}^{11} V_{y_m} + \Delta_{7m}^{11} \phi_{x_m} = \frac{4\Omega^2}{a} \sum_{n=1}^{\infty} \frac{(-1)^{m+n} \left(\left(\nu \tilde{\alpha}_m^2 + \tilde{\beta}_n^2\right) V_{x_n} + \left((1-\nu)^2 \tilde{\alpha}_m^2 \tilde{\beta}_n^2 + \nu \Omega^4\right) \phi_{y_n} \right)}{(\tilde{\beta}_n^2 + \tilde{p}_{1m}^2)(\tilde{\beta}_n^2 + \tilde{p}_{2m}^2)} \tag{C.13}$$

where sequences Δ_{jm}^{11} ($j = 1, 2, \ldots, 8$) can be obtained from Δ_{jm} (see appendix **B**) by interchanging the symbols following the scheme

$$\alpha_m \to \tilde{\alpha}_m; \beta_m \to \tilde{\beta}_m; \ q_{jm} \to \tilde{q}_{jm}; \ p_{jm} \to \tilde{p}_{jm}; \ \coth q_{jm}a \to \tanh \tilde{q}_{jm}a; \coth p_{jm}b \to \tanh \tilde{p}_{jm}b \tag{C.14}$$

Appendix D. Coefficient matrices for the force-displacement relationships of the doubly-symmetric component case ($k=j=0$).

$$\mathbf{A}^{clamped} = \begin{bmatrix} -\dfrac{\cot\Omega a + \coth\Omega a}{2\Omega^3} & -\dfrac{1}{b\Omega^4} & \cdots & 0 & \dfrac{(-1)^n}{bp_{1n}^2 p_{2n}^2} & \cdots \\[2ex] -\dfrac{1}{a\Omega^4} & -\dfrac{\cot\Omega b + \coth\Omega b}{2\Omega^3} & \cdots & \dfrac{(-1)^n}{aq_{1n}^2 q_{2n}^2} & 0 & \cdots \\[2ex] \cdots & \cdots & \cdots & \cdots & \cdots & \cdots \\[0.5ex] 0 & \dfrac{2(-1)^m}{bq_{1m}^2 q_{2m}^2} & \cdots & -\dfrac{\Delta_{2m}\delta_{mn}}{2\Omega^2} & \dfrac{2(-1)^{m+n}}{b(\alpha_n^2+q_{1m}^2)(\alpha_n^2+q_{2m}^2)} & \cdots \\[2ex] \dfrac{2(-1)^m}{ap_{1m}^2 p_{2m}^2} & 0 & \cdots & \dfrac{2(-1)^{m+n}}{a(\beta_n^2+p_{1m}^2)(\beta_n^2+p_{2m}^2)} & -\dfrac{\Delta_{4m}\delta_{mn}}{2\Omega^2} & \cdots \\[2ex] \cdots & \cdots & \cdots & \cdots & \cdots & \cdots \end{bmatrix} \quad (D.1)$$

$$\mathbf{A}^{mix1} = \begin{bmatrix} \dfrac{\coth\Omega a - \cot\Omega a}{2\Omega} & 0 & \cdots & 0 & \dfrac{\nu\alpha_n^2(-1)^n}{bp_{1n}^2 p_{2n}^2} & \cdots \\[2ex] 0 & \dfrac{\coth\Omega b - \cot\Omega b}{2\Omega} & \cdots & \dfrac{\nu\beta_n^2(-1)^n}{aq_{1n}^2 q_{2n}^2} & 0 & \cdots \\[2ex] \cdots & \cdots & \cdots & \cdots & \cdots & \cdots \\[0.5ex] 0 & \dfrac{2(-1)^m \beta_m^2}{bq_{1m}^2 q_{2m}^2} & \cdots & -\dfrac{\Delta_{1m}\delta_{mn}}{2\Omega^2} & \dfrac{2(-1)^{m+n}\left(\beta_m^2+\nu\alpha_n^2\right)}{b(\alpha_n^2+q_{1m}^2)(\alpha_n^2+q_{2m}^2)} & \cdots \\[2ex] \dfrac{2(-1)^m \alpha_m^2}{ap_{1m}^2 p_{2m}^2} & 0 & \cdots & \dfrac{2(-1)^{m+n}\left(\alpha_m^2+\nu\beta_n^2\right)}{a(\beta_n^2+p_{1m}^2)(\beta_n^2+p_{2m}^2)} & -\dfrac{\Delta_{3m}\delta_{mn}}{2\Omega^2} & \cdots \\[2ex] \cdots & \cdots & \cdots & \cdots & \cdots & \cdots \end{bmatrix} \quad (D.2)$$

$$\mathbf{A}^{mix2} = \begin{bmatrix} \dfrac{\cot\Omega a - \coth\Omega a}{2\Omega} & 0 & \cdots & 0 & \dfrac{\alpha_n^2(-1)^{n+1}}{bp_{1n}^2 p_{2n}^2} & \cdots \\[2ex] 0 & \dfrac{\cot\Omega b - \coth\Omega b}{2\Omega} & \cdots & \dfrac{\beta_n^2(-1)^{n+1}}{aq_{1n}^2 q_{2n}^2} & 0 & \cdots \\[2ex] \cdots & \cdots & \cdots & \cdots & \cdots & \cdots \\[0.5ex] 0 & \dfrac{2\nu(-1)^{m+1}\beta_m^2}{bq_{1m}^2 q_{2m}^2} & \cdots & -\dfrac{\Delta_{6m}\delta_{mn}}{2\Omega^2} & \dfrac{2(-1)^{m+n+1}\left(\nu\beta_m^2+\alpha_n^2\right)}{b(\alpha_n^2+q_{1m}^2)(\alpha_n^2+q_{2m}^2)} & \cdots \\[2ex] \dfrac{2\nu(-1)^{m+1}\alpha_m^2}{ap_{1m}^2 p_{2m}^2} & 0 & \cdots & \dfrac{2(-1)^{m+n+1}\left(\nu\alpha_m^2+\beta_n^2\right)}{a(\beta_n^2+p_{1m}^2)(\beta_n^2+p_{2m}^2)} & -\dfrac{\Delta_{8m}\delta_{mn}}{2\Omega^2} & \cdots \\[2ex] \cdots & \cdots & \cdots & \cdots & \cdots & \cdots \end{bmatrix} \quad (D.3)$$

$$\mathbf{A}^{free} = \begin{bmatrix} \dfrac{\Omega(\cot\Omega a + \coth\Omega a)}{2} & \dfrac{\nu}{b} & \cdots & 0 & \dfrac{\nu\Omega^4(-1)^{n+1}}{bp_{1n}^2 p_{2n}^2} & \cdots \\[2ex] \dfrac{\nu}{a} & \dfrac{\Omega(\cot\Omega b + \coth\Omega b)}{2} & \cdots & \dfrac{\nu\Omega^4(-1)^{n+1}}{aq_{1n}^2 q_{2n}^2} & 0 & \cdots \\[2ex] \cdots & \cdots & \cdots & \cdots & \cdots & \cdots \\[0.5ex] 0 & \dfrac{2\nu\Omega^4(-1)^{m+1}}{bq_{1m}^2 q_{2m}^2} & \cdots & \dfrac{\Delta_{5m}\delta_{mn}}{2\Omega^2} & \dfrac{2(-1)^{m+n+1}\left((1-\nu)^2\beta_m^2\alpha_n^2+\nu\Omega^4\right)}{b(\alpha_n^2+q_{1m}^2)(\alpha_n^2+q_{2m}^2)} & \cdots \\[2ex] \dfrac{2\nu\Omega^4(-1)^{m+1}}{ap_{1m}^2 p_{2m}^2} & 0 & \cdots & \dfrac{2(-1)^{m+n+1}\left((1-\nu)^2\alpha_m^2\beta_n^2+\nu\Omega^4\right)}{a(\beta_n^2+p_{1m}^2)(\beta_n^2+p_{2m}^2)} & \dfrac{\Delta_{7m}\delta_{mn}}{2\Omega^2} & \cdots \\[2ex] \cdots & \cdots & \cdots & \cdots & \cdots & \cdots \end{bmatrix} \quad (D.4)$$

where δ_{mn} is Kronecker's symbol.

Appendix E. The Wittrick-Williams algorithm and its implementation.

The dynamic stiffness (DS) matrix of this paper is used for free vibration analysis of plate-like structures. A reliable method to achieve this, i.e., to compute the natural frequencies is to apply the well-known algorithm of Wittrick and Williams (often referred to as WW algorithm) [40] which has featured in literally hundreds of papers. Before applying the algorithm, the DS matrices of all individual elements in a structure are to be assembled (in the same way as the finite element method except that there are no separate mass and stiffness matrices) to form the overall DS matrix $\mathbf{K}_f$ of the final structure, which may, of course, consist of a single element, as a special case. For instance, the reduced DS matrix $\mathbf{K}_{aa}$ of Eq. (64) may be considered as the overall DS matrix $\mathbf{K}_f$. The algorithm monitors the Sturm sequence properties of $\mathbf{K}_f$ in such a way that there is no possibility of missing any natural frequency. This is, of course, not possible in the conventional finite element or in any other approximate methods. Another point needs to be emphasised before going into the details of WW algorithm is that a new procedure which will be explained later has been introduced when applying the WW algorithm, which provides an added advantage to its application. But first the essential features of the WW algorithm are briefly explained below.

Suppose that ω denotes the circular (or angular) frequency of a vibrating structure. Then according to the WW algorithm, j, the number of natural frequencies passed, as ω is increased from zero to ω^*, is given by

$$j = j_0 + s\{\mathbf{K}_f\} \tag{E.1}$$

where $\mathbf{K}_f$, the overall DS matrix of the final structure whose elements all depend on ω is evaluated at $\omega = \omega^*$; $s\{\mathbf{K}_f\}$ is the number of negative elements on the leading diagonal of $\mathbf{K}_f^\Delta$, $\mathbf{K}_f^\Delta$ is the upper triangular matrix obtained by applying the usual form of Gauss elimination to $\mathbf{K}_f$, and j_0 is the number of natural frequencies of the structure still lying between $\omega = 0$ and $\omega = \omega^*$ when the displacement components to which $\mathbf{K}_f$ corresponds are all zeros. (Note that the structure can still have natural frequencies when all its nodes are clamped because exact member equations allow each individual member to displace between nodes with an infinite number of degrees of freedom, and hence infinite number of natural frequencies between nodes.) Thus

$$j_0 = \sum j_m \tag{E.2}$$

where j_m is the number of natural frequencies between $\omega = 0$ and $\omega = \omega^*$ for an individual component member with its ends fully clamped, while the summation extends over all members. Now with the knowledge of equations (E.1) and (E.2), it is possible to ascertain how many natural frequencies lie below an arbitrarily chosen trial frequency ω^*. This simple feature of the algorithm (with the fact that successive trial frequencies can be chosen) can be used to converge on any required natural frequency to any desired accuracy.

It should be noted that j_0 count is an essential part of the algorithm which can sometimes becomes a difficult task to compute when applying the algorithm. The difficulty in computing j_0 can be circumvented either by an indirect method [41] or by using a sufficiently finer mesh to ensure that j_0 is always zero within the frequency range of interest [26-32]. The first approach works for simple problems, e.g., when using beam structures, whilst the latter approach understandably increases the computational time.

The cumbersome issue of resolving the j_0 count problem is successfully addressed in this paper by virtue of the usefulness of the rich degrees of freedom arising from the nature of the formulation. It is well-known that the WW algorithm is based on the Rayleigh theorem [39] in which the sign count is related to the number of constraints and the degrees of freedom of the system. Specifically, for a fixed trial frequency ω^*, the sign count remains unchanged or increases by one when one constrain is removed from the structure, or in other words, this will happen when one extra degree of freedom is added to the structure. The strategy of using sufficiently finer mesh in the structure essentially increases the number of degrees of freedom and thus providing enough degrees of freedom to allow the removal of constraints and thereby making the algorithm dependent only on the sign count $s\{\mathbf{K}_f\}$ of Eq. (E.1). In the present case, the degrees of freedom in the displacement vector are actually the (Fourier) coefficients of the sine and cosine functions which are superposed to form the displacement/rotation functions on the boundaries. To put it another way, for each line node (boundary), there are more than one degree of freedom for each displacement function in terms of Fourier coefficients. Therefore, when applying WW algorithm, enough number of terms in the series expansion can be included so that the j_0 count becomes zero for a given trial frequency ω^*. This is similar, in a way, to the other strategy of using sufficiently finer mesh to increase the degree of freedom. Nevertheless, the difference between the present method and the former method lies in the fact that sufficient number of degrees of freedom is already embedded in the series-form of the general solutions used, and thus there is no need to increase the number of elements artificially to create a finer mesh. From a general but qualitative perspective, a numerical simulation suggests that even when only two or three terms of the series expansions are included in the formulation, the sign count can capture the first few natural frequencies of a plate without the need to compute the j_0 term of Eq. (E.1). However, this is simply an indicative guidance, not a prescriptive solution to the j_0 problem and caution must be exercised and each case has to be treated on its merits.

The mode shape computation is a bit more complicated than the usual procedure generally adopted for other problems because of the use of the Fourier series and the mixed formulation for the present problem. Here we start by using the reduced dynamic stiffness matrix of Eq. (64) and once an arbitrary value to a carefully chosen degree of freedom is assigned, the rest of the values in the displacement vector can be determined in terms of the given one by solving the algebraic system. The displacement, rotation, moment and shear force functions on the four boundaries of the plate can then be recovered by substituting these values into Eq. (17) to obtain the vectors $\mathbf{d}^{kj}$ and $\mathbf{f}^{kj}$. Then the unknown coefficients can be calculated using Eqs. (34) and (35) which in turn when substituted into Eq. (10) will recover the mode shapes.

References

[1] E.F.F. Chladni, Die Akustik, Breitkopf and Hrtel, Leipzig, 1802.

[2] S.D. Poisson, L'equilibre et le movements de corps elastiques. Memoares L'Academic Royale Sciences L'Institute de France 8 (1829) 357-570.

[3] Lord Rayleigh, Theory of Sound Volume 1, Macmillan, London, 1877, reprinted 1945.

[4] W. Ritz, Uber eine neue methode zur losung gewisser variations problem der mathematischen physic. Journal fur Reine und Angewandte Mathematik 135 (1909) 1-61. doi: 10.1515/crll.1909.135.1

[5] S. Timoshenko, Vibration Problems in Engineering, D. Van Nostrand Company, Inc., New York, 1937.

[6] S. Iguchi, Die Eigenschwingungen mit Klangfiguren der freien recteckigen Platte, Ing.-Archiv 21(5-6) (1953) 303-322. doi: 10.1007/BF00535853

[7] A.W. Leissa, Vibration of plates, Washington, National Aeronautics and Space Administration, Tech. Rep. NASA SP-160, 1969.

[8] A.W. Leissa, The free vibration of rectangular plates. Journal of Sound and Vibration 31 (1973) 257-293. doi: 10.1016/S0022-460X(73)80371-2

[9] G.B. Warburton, The vibration of rectangular plate. Proceedings of the Institution of Mechanical Engineers Series A 168 (12) (1954) 371-384. doi:10.1243/PIME_PROC_1954_168_040_02

[10] D.J. Gorman, Free vibration analysis of the completely free rectangular plate by the method of superposition. Journal of Sound and Vibration 57 (3) (1978) 437-447. doi:10.1016/0022-460X(78)90322-X

[11] S. Azimi, J.F. Hamilton, W. Soedel, The receptance method applied to the free vibration of continuous rectangular plates. Journal of Sound and Vibrations 93 (1) (1984) 9-29. doi: 10.1016/0022-460X(84)90348-1

[12] R.B. Bhat, Natural frequencies of rectangular plates using characteristic orthogonal polynomials in Rayleigh-Ritz method. Journal of Sound and Vibrations 102 (4) (1985) 493-499. doi: 10.1016/S0022-460X(85)80109-7

[13] Y.K. Cheng, J. Kong, The application of a new finite strip to the free vibration of rectangular plates of

varying complexity. Journal of Sound and Vibrations 181 (2) (1995) 341-353. doi: 10.1006/jsvi.1995.0144

[14] Y.F. Xing, B. Liu, New exact solutions for free vibrations of rectangular thin plates by symplectic dual method. Acta Mech. Sin. 25 (2009) 265-270. doi: 10.1007/s10409-008-0208-4

[15] Y.F. Xing, B. Liu, New exact solutions for free vibrations of thin orthotropic rectangular plates. Comp. Strut. 89 (2009) 567-574. doi: 10.1016/j.compstruct.2008.11.010

[16] R. Szilard, Theory and analysis of plates: Classical and numerical methods, Prentice-Hall, Englewood Cliffs, NJ, 1974.

[17] S. Timoshenko, S. Woinowsky-Krieger, Theory of plates and shells, McGraw-Hill, New York, 1959.

[18] W. Soedel, Vibration of shells and plates, Marcel Dekker, New York, 1993.

[19] J.R. Banerjee, Coupled bending-torsional dynamic stiffness matrix for beam elements. Int J Numer Methods Eng. 28 (1989) 1283–98. doi: 10.1002/nme.1620280605

[20] J.R. Banerjee, Free vibration analysis of a twisted beam using the dynamic stiffness method. Int J Solids Struct. 38(38–39) (2001) 6703–22. doi: 10.1016/S0020-7683(01)00119-6

[21] J.R. Banerjee, C.W. Cheung, R. Morishima, M. Perera, J. Njuguna, Free vibration of a three-layered sandwich beam using the dynamic stiffness method and experiment. Int J Solids Struct. 44(22–23) (2007) 7543–63. doi: 10.1016/j.ijsolstr.2007.04.024

[22] M.S. Anderson, F.W. Williams, BUNVIS-RG: exact frame buckling and vibration program with repetitive geometry and substructuring. J Spacecraft Rockets 24 (1987) 353–61. doi: 10.2514/3.25924

[23] B. Akkeson, BFVIBAT-A computer program for plane frame vibration analysis by an exact method. Int J Numer Methods Eng. 10 (1976) 1221–31. doi: 10.1002/nme.1620100603

[24] W.H. Wittrick, F.W. Williams, Buckling and vibration of anisotropic or isotropic plate assemblies under combined loadings. Int J Mech Sci. 16(4) (1974) 209–39. doi: 10.1016/0020-7403(74)90069-1

[25] F.W. Williams, M.S. Anderson. Incorporation of Lagrange multipliers into an algorithm for finding exact natural frequencies or critical buckling loads. Int J. Mech Sci 25(8) (1983) 579–84. DOI: 10.1016/0020-7403(83)90049-8

[26] M.S. Anderson, F.W. Williams, C. Wright, Buckling and vibration of any prismatic assembly of shear and compression loaded anisotropic plates with an arbitrary supporting structure. International Journal of Mechanical Sciences 25 (8) (1983) 585– 596. doi: 10.1016/0020-7403(83)90050-4

[27] F.W. Williams, D. Kennedy, M.S. Anderson. Analysis features of VICONOPT, an exact buckling and vibration program for prismatic assemblies of anisotropic plates. Proceeding of the 31st AIAA/ASME/ASCE/AHS/ASC structures, structural dynamics and materials conference, Long Beach, California AIAA Paper 90-0970; 1990. p. 920–90.

[28] M. Boscolo, J.R. Banerjee, Dynamic stiffness elements and their applications for plates using first order shear deformation theory, Computers and Structures 89 (2010) 395– 410. doi: 10.1016/j.compstruc.2010.11.005

[29] M. Boscolo, J.R. Banerjee, Dynamic stiffness formulation for composite Mindlin plates for exact modal analysis of structures. Part I: theory. Computers and Structures 96 (97) (2012) 61–73. doi: 10.1016/j.compstruc.2012.01.002

[30] M. Boscolo, J.R. Banerjee, Dynamic stiffness formulation for composite Mindlin plates for exact modal analysis of structures. Part II: results and applications. Computers and Structures 96(97) (2012) 73 – 84. (doi: 10.1016/j.compstruc.2012.01.003

[31] F. Fazzolari, M. Boscolo, J.R. Banerjee, An exact dynamic stiffness element using a higher order shear deformation theory for free vibration analysis of composite plate assemblies, Composite Structures 96 (2013) 262– 278. doi: 10.1016/j.compstruct.2012.08.033

[32] M. Boscolo, J.R. Banerjee, Layer-wise dynamic stiffness solution for free vibration analysis of laminated composite plates. J. Sound and Vibraion 333 (2014) 200-227. doi: 10.1016/j.jsv.2013.08.031

[33] J.R. Banerjee, Dynamic stiffness formulation for structural elements: a general approach. Comput Struct. 63(1) (1997) 101–103. doi: 10.1016/S0045-7949(96)00326-4

[34] V.V. Meleshko, Biharmonic problem in a rectangle. Applied Scientific Research 58 (1998) 217-249. doi: 10.1023/A:1000783619393

[35] V.V. Meleshko, Bending of an elastic rectangular clamped plate: exact versus 'engineering' solutions. Journal of Elasticity 48 (1997) 1-50. doi: 10.1023/A:1007472709175

[36] S.O. Papkov, V.V. Meleshko, Vibrations of rectangular plate with free edges. (in Russian). Theoretical and Applied Mechanics, Donetsk. 46 (2009) 104-112.

[37] B.M. Koialovich, Studies on the infinite systems of the linear equations (in Russian). Izv. Fiz. Mat. Inst. Steklova 3 (1930) 41-167.

[38] S.O. Papkov, The generalization of Koialovich's asymptotic law on a case of the nonnegative infinite matrix (in Russian). Din. Sist. Simferopol 1 (29) (2011) 255-267.

[39] L.V. Kantorovich, V.L. Krylov, Approximate Methods Higher Analysis, The Netherlands, Groningen, Noordhooff, 1964.

[40] W.H. Wittrick, F.W. Williams, A general algorithm for computing natural frequencies of elastic structures. Quarterly Journal of Mechanics and Applied Sciences 24(3) (1970) 263–284. doi: 10.1093/qjmam/24.3.263

[41] J.R. Banerjee, F.W. Williams, Clamped-clamped natural frequencies of a bending-torsion coupled beam. Journal of Sound and Vibration 176(3) (1994) 301-306. doi: 10.1006/jsvi.1994.1378

[42] N.W. Bazley, D.W. Fox, J.T. Stadter, Upper and lower bounds for the frequencies of rectangular clamped plates. The Johns Hopkins Univ., Appl. Phys. Lab., Tech. Memo. TG-626, 1965.

[43] R.W. Claassen, C.J. Thorne, Transverse Vibrations of Thin Rectangular Isotropic Plates. U.S. Naval Ordnance Test Sta., China Like, Calif., NOTS Tech. Pub. 2379, NAVWEPS Rept. 7016, 1960.

[44] J.W. Demmel, Applied numerical linear algebra, SIAM, Philadelphia, 1997.